Radar Remote Sensing of Agricultural Canopies: A Review

Susan C. Steele-Dunne, Heather McNairn, Alejandro Monsivais-Huertero, *Senior Member, IEEE*, Jasmeet Judge, *Senior Member, IEEE*, Pang-Wei Liu, *Member, IEEE*, and Kostas Papathanassiou, *Fellow, IEEE*

***Abstract*—Observations from spaceborne radar contain considerable information about vegetation dynamics. The ability to extract this information could lead to improved soil moisture retrievals and the increased capacity to monitor vegetation phenology and water stress using radar data. The purpose of this review paper is to provide an overview of the current state of knowledge with respect to backscatter from vegetated (agricultural) landscapes and to identify opportunities and challenges in this domain. Much of our understanding of vegetation backscatter from agricultural canopies stems from SAR studies to perform field-scale classification and monitoring. Hence, SAR applications, theory, and applications are considered here too. An overview will be provided of the knowledge generated from ground-based and airborne experimental campaigns that contributed to the development of crop classification, crop monitoring, and soil moisture monitoring applications. A description of the current vegetation modeling approaches will be given. A review of current applications of spaceborne radar will be used to illustrate the current state of the art in terms of data utilization. Finally, emerging applications, opportunities and challenges will be identified and discussed. Improved representation of vegetation phenology and water dynamics will be identified as essential to improve soil moisture retrievals, crop monitoring, and for the development of emerging drought/water stress applications.**

***Index Terms*—Agriculture, airborne radar, scattering, spaceborne radar, synthetic aperture radar, vegetation.**

Manuscript received July 8, 2016; revised October 25, 2016; accepted November 28, 2016. The work of S. C. Steele-Dunne was supported by a Vidi Grant 14126 from the Dutch Technology Foundation STW, which is part of the Netherlands Organisation for Scientific Research (NWO), and which is partly funded by the Ministry of Economic Affairs, and the work of A. Monsivais-Huertero was supported by the National Council of Science and Technology of Mexico (CB-2010-155375). *(Corresponding author: Susan Catherine Steele-Dunne.)*

S. C. Steele-Dunne is with the Department of Water Resources, Faculty of Civil Engineering and Geosciences, Delft University of Technology, 2628 CN Delft, The Netherlands (e-mail: s.c.steele-dunne@tudelft.nl).

H. McNairn is with the Agriculture and Agri-Food Canada, Science and Technology Branch, Ottawa ON K1A 0C6, Canada (e-mail: heather.mcnairn@agr.gc.ca).

A. Monsivais-Huertero is with the Escuela Superior de Ingeniera Mecanica y Electrica, Ticoman, Instituto Politecnico Nacional, 07738 Mexico City, Mexico (e-mail: monsivais@ufl.edu).

P.-W. Liu and J. Judge are with the Center for Remote Sensing, Department of Agricultural and Biological Engineering, Institute of Food and Agricultural Sciences, University of Florida, Gainesville, FL 32611 USA (e-mail: bonwei@ufl.edu; jasmeet@ufl.edu).

K. Papathanassiou is with the Information Retrieval Group, Radar Concepts Department, Microwaves and Radar Institute, German Aerospace Center, 82234 Wessling, Germany (e-mail: kostas.papathanassiou@dlr.de).

Color versions of one or more of the figures in this paper are available online at http://ieeexplore.ieee.org.

Digital Object Identifier 10.1109/JSTARS.2016.2639043

I. Introduction

SEVERAL recent studies suggest that backscatter data, at C-band and higher frequencies, contains a lot more information on vegetation dynamics than that currently used (e.g., [1]–[3]), with potential implications for agricultural monitoring. Radar backscatter from a vegetated surfaces comprises contributions of direct backscatter from the vegetation itself, backscatter from the soil that is attenuated by the canopy and backscatter due to interactions between the vegetation and the underlying soil [4]–[6]. The interactions between microwaves and the canopy are influenced by the properties of the radar system itself, namely the frequency and polarization of the microwaves, and the incident and azimuth angles at which the canopy is viewed (e.g., [7]–[10]). Interactions between microwaves and the canopy are governed by the dielectric properties, size, shape, orientation, and roughness of individual scatterers (i.e., the leaves, stems, fruits, etc.) [11]–[13], [14] and their distribution throughout the canopy [15]–[17]. The dielectric properties of vegetation materials depend primarily on their water content and to a lesser degree on temperature and salinity [18], [19]. These crop-specific canopy characteristics vary during the growing season, and are influenced by environmental conditions and stress [20]–[28]. Scattering from the underlying soil is influenced by its roughness and dielectric properties (e.g., [29] and [30]), which depend primarily on its moisture content (e.g., [31] and [32]). Consequently, there is significant potential for the use of radar remote sensing in agricultural applications, particularly classification, crop monitoring, and soil/vegetation moisture monitoring. Furthermore, the ability of low-frequency microwaves (1–10 GHz) to penetrate cloud cover, and to allow day and night imaging, ensures timely and reliable observations [33].

Currently, most crop classification and crop monitoring activities rely on spaceborne SAR data due to their finer spatial resolution [34]–[37]. The difficulty in using scatterometry for crop classification is the mismatch between the resolution requirements for agricultural applications (from meters in precision agriculture to kilometers for large-scale monitoring) and the spatial resolution attainable with spaceborne scatterometers. These typically have resolutions of tens of kilometers and are, therefore, better suited to large-scale vegetation classification and monitoring [38]–[43]. For soil moisture, on the other hand, both SAR and scatterometry have been used successfully. High (spatial) resolution SAR observations from Advanced Land Observing Satellite (ALOS)-PALSAR proved sensitive to soil

moisture (e.g., [44]), however the limited revisit time means that they are not suitable for many applications. NASA's Soil Moisture Active Passive (SMAP) mission [45] planned to combine passive radiometry with SAR measurements, but the radar instrument failed six months after launch in 2015. Soil moisture observations from advanced scatterometer (ASCAT) have been used in a wide range of climate and hydrological applications [46]–[49]. The archive of ERS1/2 data and the future operational availability of ASCAT data from MetOp constitutes a soil moisture data cornerstone for climate studies.

The goal of this manuscript is to review microwave interactions with vegetation and present a vision to facilitate the increased exploitation of the past, current and future radar data records for agricultural applications. A review will be provided of ground-based scatterometer experiments and airborne radar experiments focussed on crop classification, crop monitoring, and soil moisture retrieval. We will highlight the commonality in how vegetation is modeled for both scatterometry and SAR applications. It will be shown how this shared heritage contributed to the operational exploitation of current spaceborne scatterometer and SAR data for crop classification, monitoring and soil moisture monitoring. We will review recent research indicating that spaceborne radar observations are sensitive to vegetation dynamics at finer temporal scales than those considered in current applications. Finally, we will conclude with a vision of how the synergy between SAR and scatterometry, as well as new ground-based sensors could be utilized to facilitate the increased exploitation of spaceborne radar observations for agricultural monitoring.

II. Experimental Campaigns

This section will review the ground-based and aircraft campaigns that contributed to our current understanding of microwave interactions with vegetation in agricultural landscapes. Tower- and truck-based scatterometers are used for ground campaigns, while SAR instruments are more commonly used in airborne campaigns. Both technologies are used to investigate the sensitivity of backscatter to soil moisture, and vegetation structure and moisture content as a function of frequency, polarization, and incidence angle. This knowledge has been utilized in the design and exploitation of spaceborne scatterometry and SAR systems.

A. Ground-Based Scatterometers

Ground-based scatterometers are suitable for the collection of multitemporal datasets with high temporal resolution (diurnally, daily, or over the entire growth cycle). Data are typically collected at plot scales. Operating a tower-based instrument is a lot less expensive than flying an airborne instrument, so the data record can be a lot denser in time than that from an airborne campaign. It is also much easier to vary the observation parameters such as incidence and azimuth angle, so it is easy to compare different observation strategies. Detailed and repeated ground data can be collected at plot scales over time, and plots can be manipulated by imposing specific soil or crop treatments or by modifying moisture conditions using irrigation. Consequently, ground-based scatterometer experiments are ideal for collecting the detailed data necessary for theoretical developments and validation activities and have played a critical component of radar studies for over 40 years.

Early field experiments using ground-based scatterometers from the University of Kansas yielded important preliminary evidence of the sensitivity of radar backscatter to soil moisture and vegetation cover. The University of Kansas microwave active and passive spectrometer (MAPS) from 4 to 8 GHz was used by Ulaby and Moore to demonstrate that sensitivity to soil moisture is greatest at lower frequencies and in horizontally polarized backscatter and that rain on the soil makes the surface appear smoother [50]. MAPS was used in one of the first studies to show that the radar response to soil moisture depends on surface roughness, microwave frequency, and look angle [51]. In a subsequent study in corn, milo, soybeans, and alfalfa fields, MAPS was used to demonstrate that soil moisture could be detected through vegetation cover. They demonstrated that small incidence angles (5–15° from nadir) and horizontal polarization were best suited for monitoring soil moisture, while higher frequencies and larger incidence angles were more sensitive to vegetation, and therefore, more suited to crop identification/classification [7]. Similar results were also found with the University of Kansas MAS 8–18 GHz scatterometer [8]. Measurements using this system were used for the development and first validation of the water cloud model (WCM) [52], discussed in Section III-A. A lower frequency scatterometer, the MAS 1–8 GHz, was used to show that frequencies below 6 GHz and incidence angles less than 20° from nadir are best suited to minimize the influence of vegetation attenuation on the relationship between soil moisture and backscatter. They also showed that row direction has no impact on cross-polarized backscatter from 1 to 8 GHz, but it does influence copolarized backscatter below 4 GHz. Finally, they showed that a linear relationship could be established between soil moisture and horizontally copolarized backscatter at 4.25 GHz and an incidence angle of 10°. Even without fitting the data for individual vegetation types, a correlation coefficient as high as 0.80 has been reported. Ulaby *et al.* [53] showed that for extremely dry soils, the contribution of the vegetation was very significant but that for the dynamic range of soil moisture of interest in hydrological and agricultural applications, the influence of vegetation was "secondary" to that of soil moisture. Data from the MAS 1–8 GHz and the MAS 8–18 GHz were combined to produce a clutter model for agricultural crops [54]. Later experiments explored the complexity of the canopy. Ulaby and Wilson [55] used a truck mounted L-, C- and X-band FMCW scatterometer to show that agricultural canopies are highly nonuniform and anisotropic at microwave frequencies resulting in polarization-dependent attenuation and soil contribution to backscatter. The relative contribution of leaves and stalks to total backscatter was also shown to depend on frequency with leaves accounting for 50% of the canopy loss factor at L-band and 70% at X-band. Tavokoli *et al.* used an L-band radar to measure the attenuation and phase shift patterns of horizontally and vertically polarized waves transmitted through a fully grown corn canopy in order to develop and evaluate a model for radar interaction with

agricultural canopies, explicitly accounting for the regular plant spacing and row geometry [56].

Meanwhile, the radar observation of vegetation (ROVE) experiments in the Netherlands [57] were focused on the potential of using radar observations in agricultural mapping, monitoring, and yield forecasting. An X-band FMCW scatterometer was mounted on a carriage that could be moved along fields with a rail system and used to measure at a range of incidence angles from 15 to 80°. This system was used to measure multiple crops, each growing season from 1974 to 1980. Limited airborne observations were also made using a side-looking airborne radar (SLAR). One of the primary aims was the identification and classification of crops from SLAR images. Krul [58] used the ROVE data to show that during the growing season, the dynamic range of X-band backscatter of several crops varied between 3 and 15 dB, underscoring the importance of accurate calibration. In particular, combining incidence angles was mooted as one solution to separate the influences of soil moisture and vegetation. Bouman and Kasteren [59] highlighted the importance of geometry, showing that changes in canopy architecture due to strong winds could lead to differences of 1–2 dB. In sugar beets, the architectural changes in the plants in the transition from saplings to fully grown plants made it possible to monitor their growth up to a fractional cover of about 80% and a biomass of 2–3 ton/ha. A thinning experiment, in which some of the plants were removed, suggested that changes in cover due to pest/disease during the season would be difficult to detect. In barley, wheat, and oats, Bouman and Kasteren [60] showed that the interannual variability in backscatter could be as much as the range due to growth. Nonetheless, X-band backscatter could be useful for the classification and detection of some, though not all, developmental phases. In particular, soil moisture variations confounded the detection of emergence and harvest. Bouman [61] suggested that multifrequency observations might be useful to separate the backscatter contributions from potato, barley, and wheat thereby improving the estimation of dry canopy biomass, canopy water content, fractional cover, and crop height.

Ground-based scatterometer experiments have been used extensively, especially in early SAR research, to gain an understanding of responses as targets change and SAR configurations are modified. They allowed scientists to develop and test methodologies prior to the engineering of SAR satellite systems, and before space-based data became available. In addition to collecting data for model development and testing, scatterometers can also be used in novel ways to study phenomenon not easily implemented using air- or space-borne systems. Inoue *et al.* [62] used a multifrequency polarimetric scatterometer to measure backscatter over a rice field once per day for an entire growing season in order to relate the microwave backscatter signature to rice canopy growth variables. They investigated the influence of rice growth cycle on backscatter at L-, C-, X-, Ku-, and Ka-bands for a range of incident and azimuth angles and their relationship to leaf area index (LAI), stem density, crop height, and fresh biomass. The Canada Centre for Remote Sensing (CCRS) acquired a ground-based scatterometer in 1985, which was dedicated primarily to agriculture research. This was a three-band system mounted on a hydraulic boom supported on the flat bed of a 5-ton truck. The scatterometer acquired data at L, C, and Ku bands (1.5, 5.2, and 12.8 GHz) and at four polarizations: HH, VV, HV, VH. The boom allowed a change in incident angle, with operations typically at 20°–50°.

Some of the earliest research using the CCRS scatterometer looked at crop separability. Brisco *et al.* [63] reported the best configurations for this purpose, i.e., higher frequencies (Ku-band as opposed to C- or L-bands), the cross polarization, shallower incident angles, and observations during crop seed development. These conclusions have been reinforced by many subsequent studies, whether using airborne- or satellite-based SAR observations. The diurnal effects of backscatter were tracked by Brisco *et al.* [64]. Backscatter was sensitive to daily movement of water, mostly due to the diurnal pattern of water in plants during active growth, and due to the diurnal pattern of soil moisture during periods of crop senescence. Toure *et al.* [65] modified the MIMICS model to accommodate agricultural parameters and used the scatterometer to validate the accuracy of this modified model to estimate soil moisture as well as stem heights and leaf diameters.

Investigations into the sensitivity of backscatter to soil moisture, crop residue, and tillage were a focus of a number of scatterometer investigations. Major *et al.* [66] found that backscatter was sensitive to soil moisture even in the presence of short-grass prairie conditions. Meanwhile Boisvert *et al.* [67] modeled the effective penetration depth for L-, C-, and Ku-bands, an important consideration in validation of soil moisture retrievals even with current satellite systems. Data from the scatterometer allowed Boisvert *et al.* [67] to forward model soil moisture for various models [Oh, Dubois, and the integral equation model (IEM)] and to evaluate the performance of these models against field data. Assessment of model approaches was also a focus of scatterometer research, with McNairn *et al.* [68] using a dual incident angle approach to estimate both soil moisture and roughness.

Canadian researchers also imposed tillage and residue treatments on field plots, irrigating these plots to simulate various wetness conditions. These studies confirmed that residue is not transparent to microwaves when sufficiently wet, and that in fact cross polarizations can be very sensitive to the amount of residue present [69], [70]. Airborne and satellite data often detect "bow-tie" effects on agricultural fields due to tillage, planting, and harvesting direction. This was also reported by Brisco *et al.* [71] but this study was one of the first to reveal that the cross polarization is much less affected by look direction. This is an important consideration for agriculture given that significant errors in soil moisture retrievals can be introduced by this effect [67].

The development of a retrieval algorithm for NASA's SMAP mission spurred several ground-based radar experiments [72]. NASA's ComRAD system is a truck-based SMAP simulator that includes a dual-pol 1.4-GHz radiometer and a 1.24–1.34-GHz radar [73]. The instrument is mounted on a 19-m hydraulic boom and is typically configured to measure at a 40° incidence angle similar to that of SMAP, though it can sweep in both azimuth and incidence angle. Early deployments focussed on forest attenuation of the soil moisture signal (see [74] and [75]).

O'Neill *et al.* [76] collected active and passive L-band observations over a full growing season in adjacent corn and soybean fields to refine the SMAP retrieval algorithms. In particular, these data yield insight into the influence of changing vegetation conditions and the relationship between contemporaneous active and passive observations. Srivastava *et al.* [77] used this data to compare different approaches to estimate vegetation water content (VWC). The combined active/passive ComRAD system meant that they could compare backscatter in different polarizations, polarization ratios, radar vegetation index (RVI), and microwave polarization difference index. They found that at L-band, an HV backscatter was the best estimator for VWC. This is a valuable result as it obviates the need for ancillary data, like NDVI and a parameterization to provide VWC for the retrieval algorithm.

The University of Florida L-band Automated Radar System (UF-LARS) [78] operates at 1.25 GHz and can be used to observe VV, HH, HV, and VH backscatter every 15 min for several weeks. Measurements are typically made from a height of about 16 m above the ground with an incidence angle of 40°. The ability of UF-LARS to measure with such high temporal resolution and over long periods offers a unique insight into the backscatter signature of near-surface soil moisture dynamics in response to precipitation, irrigation, and other environmental conditions. The density and accuracy of data also renders it ideal for developing and validating backscattering models. The UF-LARS has been used to investigate the dominant backscattering mechanisms from bare sandy soils, to evaluate the sensitivity of backscatter to volumetric soil moisture [79] and growing vegetation [78], to investigate the benefit of combining active and passive microwave observations for soil moisture estimation [80] and to evaluate uncertainty in the SMAP downscaling algorithm for sweet corn [81]. Data from theUF-LARS were used by Monsivais-Huertero *et al.* to compare bias correction approaches used in the assimilation of active/passive microwave observations to estimate soil moisture [82].

Finally, the Hongik polarimetric scatterometer (HPS) is a quad-pol L-, C-, and X-band scatterometer that operates on a tower [83]. It has been used for model development and cross comparisons with satellite data over a number of crops [84]–[86], and to develop a modified form of the WCM in which the leaf size distribution is parameterized [87]. Inclusion of an additional antenna and modifications to the mechanical system also allow it to be configured as a rotational SAR system [88].

B. Airborne Radar Instruments

One drawback of ground-based investigations is the rapid change of the imaging geometry in range and cross range across a relatively small scene. Near-field effects (i.e., the curved wavefront interacting with tall crops) also need to be taken into account. The main limitation of using ground-based scatterometers is that they measure a single field or, at best, can be moved with a mechanical system to observe multiple fields. This greatly limits the diversity of fields and conditions that can be observed in a single campaign. Aircraft-mounted sensors allow measurements along flight lines spanning many fields, which may include different crops, roughness characteristics, growth stages, and moisture content. However, an aircraft campaign is typically limited to a few flights. Airborne radar instruments, therefore, offer a complementary perspective to that from tower-based instruments. In Europe, the 1–18-GHz DUT SCATterometer (DUTSCAT) [89] and the C-/X-band ERASME helicopter-borne scatterometer [90] were deployed over five test sites during the AGRISCATT88 campaigns that built on the knowledge and expertise gained from the ROVE experiments [91]. Bouman *et al.* [92] used the DUTSCAT data to investigate the potential of multifrequency radar for crop monitoring and soil moisture. Their analysis confirmed findings from their earlier ground-based study [61] that the sensitivity of backscatter to canopy structure complicates the retrieval of biomass, soil cover, LAI, and crop height. They also confirmed that higher frequencies (X- to K-band) were best suited to crop separability, while L-band yielded the most information on soil moisture in bare soils. Similar conclusions were drawn by Ferrazzoli *et al.* [93] from an analysis of the DUTSCAT and ERASME datasets. They used the same datasets to demonstrate that leaf dimensions had a significant influence on backscatter from agricultural canopies, particularly at S- and C-band [94]. Schoups *et al.* [95] used the DUTSCAT data to investigate the sensitivity of backscatter from a sugar beet field to soil moisture and roughness, leaf angle distribution and moisture content, canopy height, and incidence angle and frequency. Prevot *et al.* [96] used the ERASME data to develop a modified version of the WCM in which multiangle data are used to account for roughness effects, and presented an inversion approach capable of retrieving VWC where LAI is less than 3. Benallegue *et al.* [97] analyzed the ERASME data collected over the Orgeval basin (France) to evaluate the use of multifrequency, multiincidence angle radar observations for soil moisture retrieval. Their results were consistent with early results of Ulaby *et al.* in that low frequency (C-band in this case) observations 20° from nadir contained most information on soil moisture while the higher frequency (X-band) observations at larger incidence angles were used to quantify the vegetation attenuation. Benellegue *et al.* [98] subsequently used the ERASME data to argue that variability in soil dielectric constant (moisture content) and roughness precludes the use of SAR (e.g., ERS-1 SAR) to estimate soil moisture at a single field level, but that larger scale trends in the basin could be detected if the measurements were on a scale of about 1 km. These early airborne experiments demonstrated the robustness of the theories and models developed from ground-based scatterometry over larger areas and for a wider range of land cover and crop types. The international community involved in collecting both airborne data and ground data is indicative of the growing interest in using radar for crop classification and crop and soil monitoring at that time.

In the 1980s, the Canadian CV-580 SAR was developed as a multifrequency (L-, C-, and X-band) airborne system. The CV-580 was flown in support of many early agricultural experiments, demonstrating the value of SAR for crop classification, whether by integrating SAR with optical data [99] or simply using its multiple frequency capability [100]. Later the system was modified to incorporate full polarimetry on C-band [101]. This

mode was instrumental for the scientific community, providing data to develop polarimetric applications in advance of access to such data from satellites systems. These airborne data led to many early discoveries regarding the value of polarimetry. McNairn *et al.* [102] used these data to investigate polarization for crop classification, discovering that three C-band polarizations (whether linear or circular) were sufficient to accurately classify crops. In fact the best three-polarization combination included the LL circular polarization (HH-HV-LL). Data collected by the airborne CV-580 also assessed the value of polarimetry for crop condition assessment. McNairn *et al.* [103] used several linear polarizations at orientation angles of 45° and 135° and circular (RR and RL) polarizations to classify fields of wheat, canola, and peas into productivity zones, indicative of variations in crop height and density. C-band polarimetric data from the CV-580 also demonstrated that linear and circular polarizations could classify wheat fields into zones of productivity weeks before harvest [104]. These zones were well correlated with zones defined by yield monitor data.

The CV-580 was instrumental in efforts to ready the international community to exploit data from Canada's first satellite, RADARSAT-1. The GlobeSAR-1 program was initiated in 1993, two years prior to the launch of RADARSAT-1, with objectives to acquaint users with the application of this new data source and to facilitate use of imagery from the ERS-1 satellite [105]. The CV-580 travelled approximately 100 000 km, acquiring more than 125 000 km^2 of multimode SAR data over 30 sites in 12 countries including France, the U.K., Taiwan, China, Vietnam, Thailand, Malaysia, Kenya, Uganda, Jordan, Tunisia, and Morocco [106]. C- and X-band multiple polarization as well as fully polarimetric data from this campaign fuelled early research into a diversity of applications including rice identification and monitoring, soil moisture estimation, and land cover mapping [107]. In China, these data were used to develop multipolarization and multifrequency-based land cover maps with accuracies close to 90%; in Thailand CV-580 data were combined with TM and SPOT data to improve land cover discrimination. The data collected by this airborne platform and the SAR training delivered during the GlobeSAR-1 program had a lasting impact for RADARSAT applications in these regions.

By the late 1990s, its high resolution capabilities meant that SAR had been identified as the way forward in terms of crop classification and monitoring. Several airborne campaigns using experimental-SAR (E-SAR) system from the German Aerospace Center (DLR) were conducted in Europe to prepare for the availability of spaceborne radar data from Sentinel-1 and TerraSAR-X. During the TerraSAR-SIM campaign (Barrax, Spain, in 2003), DLR's airborne E-SAR system was used during five flights to quantify the impact of time lag between satellite acquisitions at different wavelengths on agricultural applications, particularly, classification and crop monitoring [108]. The data collected were used again recently to test retrievals of above ground biomass in a wheat canopy using CosmoSky-Med and Sentinel-1 SAR data [109]. The Bacchus campaign and follow-up activities also employed DLR's E-SAR system to evaluate the potential for using C- and L-band SAR in viticulture [110]. In addition to gaining insight into the scattering mechanisms in vineyards [111], the synergy of combining radar and optical imagery for classification purposes was considered [112]. E-SAR was also combined with spectral data during the AQUIFEREx campaign to produce high-resolution land maps for water resources management in Tunisia [113]. During the Eagle2006 campaign (see [114]), L-, C- and X-band data were acquired over three sites in the Netherlands. C-band images were used to simulate Sentinel-1 data, to facilitate the development and testing of retrieval algorithms. Optical and thermal imagery, as well as extensive ground measurements were also collected over grass and forest sites. E-SAR was also flown during the AgriSAR2006 campaign during which *in situ* data and satellite imagery were combined with airborne SAR and optical imagery to support decisions regarding the instrument configurations for the first Sentinel Missions [115], [116]. The data were used to investigate the impact of polarization on crop classification [37], to develop algorithms for soil moisture retrieval from SAR [10], [117], [118].

In preparation for NASA's Soil Moisture Active Passive (SMAP) mission, NASA's Jet Propulsion Laboratory developed the Passive Active L- and S-band system (PALS) instrument to investigate the benefit of combining passive and active observations. It has been deployed during several experiments in the last two decades [119], [120]. Earlier experiments such as measurements conducted in the Little Washita Watershed, OK, USA, during Southern Great Plaints experiment 1999 (SGP99), and in the Walnut Creek, IA, USA, during Soil Moisture Experiment 2002 (SMEX02) were primarily to understand the sensitivities of the multifrequency and -polarized active and passive observations. Although the studies found great sensitivities of both active and passive observations to the soil moisture, the active observations were more sensitive to the variation of vegetation conditions [121], [122]. In agreement with the earliest ground-based experiments, the L-band observations were more sensitive to the soil moisture changes due to better penetration in the agricultural region, while those from the S-band were more sensitive to the VWC.

PALS still plays a significant role in NASA-SMAP pre- and postlaunch calibration and validation activities through the so-called SMAP validation experiments (SMAPVEX) [123], [124]. Airborne PALS data been used to test and modify soil moisture retrieval algorithms in agricultural regions [120], [124], and to develop downscaling algorithms for high spatial resolution soil moisture under different levels of VWC by integrating the active and passive observations for SMAP [125], [126]. Similar to PALS, an airborne polarimetric L-band imaging SAR (PLIS) was designed and combined with the polarimetric L-band multibeam radiometer (PLMR) to support the development of soil moisture algorithms for the SMAP mission in Australia [127]–[129]. Five field campaigns, called SMAP Experiments (SMAPExs), have been conducted using PLIS from 2010 to 2015 in agricultural and forest regions in south-eastern Australia. Wu *et al.* [130], [131] used the observations from SMAPEx1-3 to validate and calibrate the SMAP simulator and to evaluate the feasibility and uncertainty of the SMAP baseline downscaling algorithms.

III. Accounting for Backscatter From Vegetation

Data collected in the experimental campaigns discussed in the previous section have been used to develop, test, and validate models to simulate the influence of the soil and vegetation on backscatter. In this section, the most common ways in which backscatter from a vegetated surface is simulated/interpreted are reviewed. The WCM, and energy and wave approaches are used for both forward modeling and inversion to obtain soil moisture, VWC or biomass and/or LAI. SAR decompositions quantify the contributions of surface, volume, and double-bounce backscatter to the total power and are particularly useful for classification and growth stage identification.

For vegetated terrain, the effects of canopy constituents, geometry, and moisture distribution are typically modeled as a scattering phase function, extinction coefficient, and scattering albedo, as described by Ulaby *et al.* [132]. The canopy can be modeled either as a continuous media with statistical dielectric variations within the canopy or as a discrete layered medium [133].

A. WCM

In 1978, Attema and Ulaby published the WCM, an approach to characterize a vegetation canopy as a collection of uniformly distributed water droplets [132]. The WCM is a zeroth-order radiative transfer solution in which the power backscattered by the entire canopy is modeled as the incoherent sum of the contributions from the canopy (as a whole) as well as the underlying soil. In this model, multiple scattering (between soil canopy and within the canopy) is ignored [52], [96]. The canopy can be represented with one or two vegetation parameters. The WCM has been adapted to model scattering from a range of crop canopies. Prevot *et al.* [96] reviewed these approaches, which have considered canopy (or leaf) water content and LAI as descriptors of the vegetation canopy. In the WCM, total backscatter σ^0 is modeled according to incoherent scattering from vegetation $\sigma^0_{\rm veg}$ and $\sigma^0_{\rm soil}$. Two-way transmission-backscatter through the canopy attenuates the signal and is modeled using an attenuation factor τ^2 as

$$\sigma^0 = \sigma^0_{\rm veg} + \tau^2 \sigma^0_{\rm soil} \tag{1}$$

$$\sigma^0_{\rm veg} = AV_1 \cos\theta (1 - \exp(-2BV_2/\cos\theta)) \tag{2}$$

$$\tau^2 = \exp(-2BV_2/\cos\theta) \tag{3}$$

where *A* and *B* are the parameters of the model and θ is the incidence angle. V_1 and V_2 are canopy descriptors. One vegetation parameter can be used for both V_1 and V_2, or alternatively different parameters can be assigned to each of V_1 and V_2. Direct scattering from the soil must be modeled within the WCM. Typically, a simple linear model has been used as Ulaby *et al.* (1978) demonstrated that scattering from the soil can be expressed as a simple linear function between backscatter and soil moisture, M_v, as

$$\sigma^0_{\rm soil} = {\rm CM}_v + D \tag{4}$$

where *C* and *D* are the slope and intercept of the relationship between backscatter and soil moisture. Some attempt has been made to use more physically based approaches to model scattering from the soil, including integration of the physically based IEM with the WCM [134].

The attraction of the WCM is that this is a relatively simple model whereby given a sufficient number of radar measurements (in multiple angles, polarizations, and/or frequencies), both the vegetation canopy parameters and soil moisture can be simultaneously estimated. However, the WCM is a semiempirical mode, whereby parameterization of the vegetation and soil variables is accomplished using experimental data. As such, performance of the model is affected by the quality and robustness of these data. The WCM has typically been parameterized on a crop-specific basis given that the vegetation structure varies significantly among different species. If multiple radar measurements are used, inversion of the WCM allows estimates of vegetation parameter(s), for example, LAI and/or VWC, as well as underlying soil moisture [96], [135], [136]. Alternatively, soil moisture data can be supplied to estimate the vegetation parameters [137], or vegetation data can be provided to estimate the soil moisture [138].

The simplicity of the WCM means that it is easy to parameterize and use for forward modeling and retrieval. However, its assumption regarding the uniform distribution of moisture in the canopy is a huge simplification of reality. Fig. 1 illustrates the dynamics of the vertical moisture content distribution in corn during a growing season from destructive data collected in the Netherlands in 2013. Fig. 1(a) shows the vegetation leaf water content in kg·m^{-2}. Each dot corresponds to the total VWC of leaves at a certain height (indicated on the *y*-axis), in one square meter. Fig. 1(b) shows the water content of the stems in kg·m^{-2}. Each dot corresponds to the total water content in all stems in the 10-cm stems centered at that height (indicated on the *y*-axis), in one square meter. Fig. 1(a) and (b) demonstrates that, in contrast to the assumption of the WCM, the moisture in the canopy is far from evenly distributed. Most of the water stored as leaf water is concentrated in the midsection where the largest leaves occur. During the vegetative stages (up to 27 July), the moisture distribution in the stem is relatively uniform, decreasing only slightly with height. When the ears start to form and separate from the stem, the stem VWC at and above the ears becomes relatively dry. The gradient in stem VWC as a function of height becomes clearer and it changes as the season progresses. The contributions of leaf, stem, and ear moisture to the total is shown in Fig. 1(c). This illustrates that the distribution of canopy water content among the different scatterers also varies during the growing season. The influence this has on backscatter depends on frequency and polarization. It is clear that the assumptions of the WCM are very simplistic compared to the actual distribution and dynamics of water content during the growing season.

B. Energy and Wave Approaches

Equation (1) can be formulated as

$$\sigma^0 = \sigma^0_{\rm soil} + \sigma^0_{\rm veg} + \sigma^0_{\rm sv} \tag{5}$$

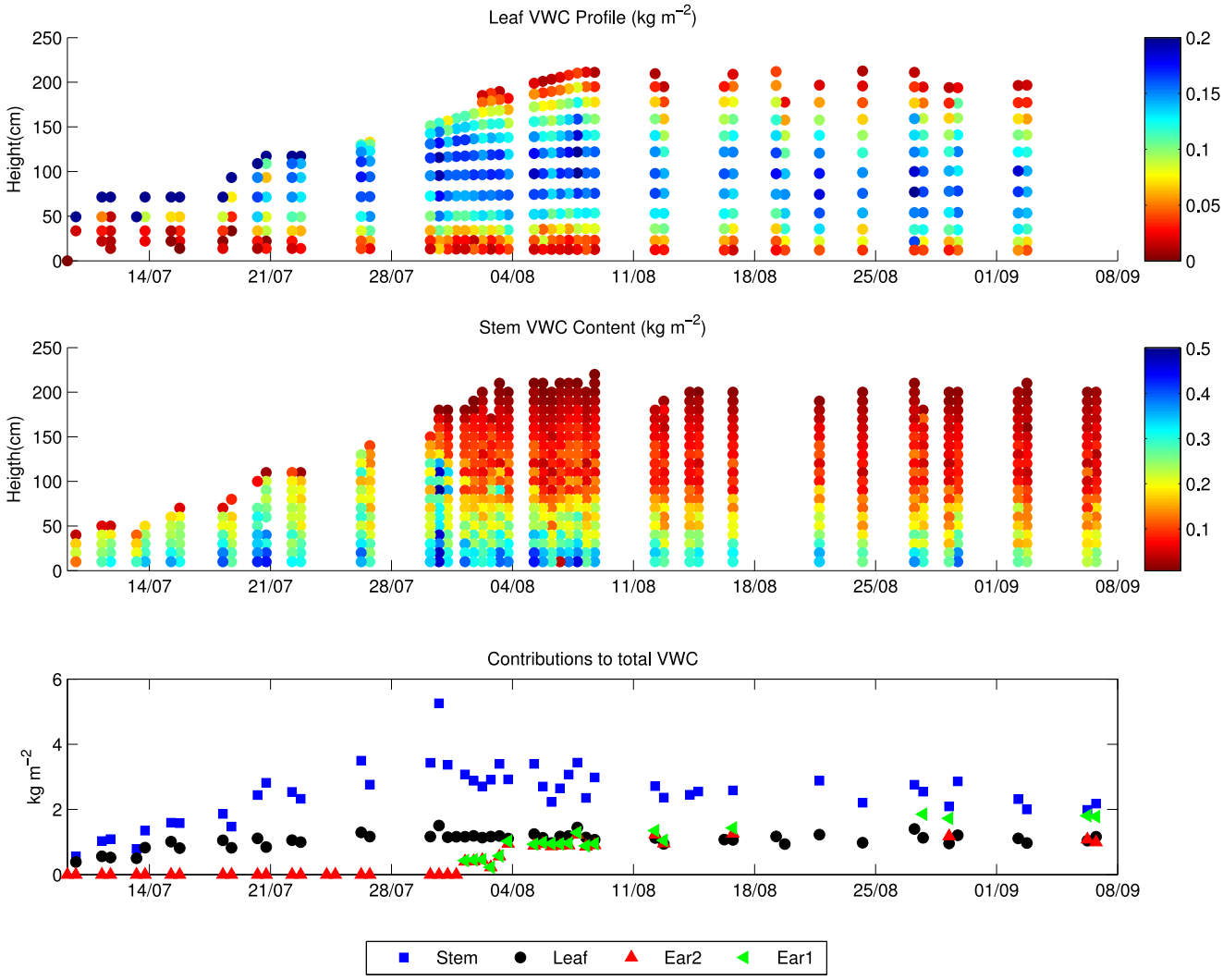

Fig. 1. Vertical distribution of (a) leaf and (b) stem moisture content, and the contributions of leaf, stems, and ears to total VWC (kg·m^2) (c) in an unstressed corn canopy.

so that the total backscatter from the vegetated surface σ^0 includes scattering contributions from the soil surface (σ^0_{soil}), direct scattering from the vegetation (σ^0_{veg}), and from interactions between soil and vegetation (σ^0_{sv}) [4]. The σ^0_{soil} is a function of the reflectivity of the soil and is highly sensitive to surface roughness. The σ^0_{veg} is a function of canopy opacity and geometry. For a mature crop, σ^0_{veg} could comprise a significant portion of σ^0 [139].

Scatterers within the layered medium are characterized by canonical geometric shapes such as ellipsoids or disks for leaves and cylinders for trunks, branches, and stems [17]. Typically, the vegetation consists of a canopy layer within which these objects are randomly arranged, a stem layer with randomly located nearly vertical cylinders that may or may not extend into the branch layer, if present, and an underlying rough ground. Several backscattering models exist for vegetated terrain, e.g., [140]–[143]. The σ^0 for the vegetated terrain can be estimated either through the energy or intensity approach or the wave approach [144].

Both the energy and the wave approaches are based on physical interactions of electromagnetic waves with vegetation. In the energy approach, only amplitudes of the electromagnetic fields are estimated. The backscattering is described either through radiative transfer (RT) equations [145], matrix doubling theory [146], or Monte Carlo simulations [147]. The RT models (e.g., Michigan microwave canopy scattering (MIMICS), [143] and the Tor-Vergata model [148]) are energy-based equations that govern the transmission of energy through the scattering medium. According to the radiative transfer theory, the propagating energy interacts with the medium through extinction and emission. Extinction causes a decrease in energy, while emission accounts for the scattering by the medium along the propagation path. For a medium with random particles, the RT theory assumes that the waves scattered from the particles are random in phase and the total scattering can be estimated by incoherent summation over all particles. Thus, the extinction and emission processes can be represented by the average extinction and source matrices within each layer. The RT models represent

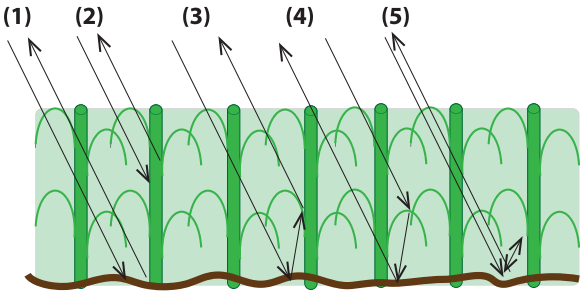

Fig. 2. Scattering mechanisms considered in the first-order models for both energy and wave based approaches: (1) direct ground (2) direct vegetation (3) ground–vegetation (4) vegetation–ground (5) ground–vegetation–ground.

a first-order solution and use Foldy's approximation to estimate a mean field as a function of height within the vegetation. This mean field is then scattered from each of the vegetation constituents. Soil surface scattering and specular reflection are denoted by scattering and reflectivity matrices. The intensities across interfaces are continuous under the assumption of a diffuse boundary condition.

The MIMICS model represents the vegetation as divided in three regions: the crown region, the trunk region, and the underlying ground region [133]. The radiative transfer equations are solved iteratively in a two-equation system; one represents the intensity vector into upward direction and the second equation represents the intensity into the downward direction. The Tor-Vergata model divides the vegetation into N layers over a dielectric rough surface. Each layer is described by the upper half-space intensity scattering matrix and the lower half space intensity scattering matrix. To compute the total scattered field from the scene, the matrix doubling algorithm is used, under the assumption of azimuthal symmetry. The first-order solution of both RT models accounts for five scattering mechanisms, as shown in Fig. 2 (1) direct scattering from soil (σ^0_{soil}); (2) direct scattering from vegetation (σ^0_{veg}); (3) ground reflection followed by vegetation specular scattering; (4) vegetation specular followed by ground reflection; and (5) double bounce by ground reflection and/or vegetation backscattering and ground reflection. The addition of the scattering mechanisms 3–5 are represented by σ^0_{sv} in (5).

Though MIMICS was originally developed for forest canopies [65], [143] modified it for use in agricultural (wheat and canola) canopies by removing the distinct trunk layer, expressing the constituents of canola and wheat in terms of cylinders, discs and rectangles, and parameterizing leaf density as a function of input LAI. A similar approach was employed by Monsivais–Huertero and Judge [139] to model a maize canopy. DeRoo *et al.* [149] adapted the MIMICS to model the soybean crop and Liu *et al.* [150] used MIMICS to assimilate the backscattering coefficient into a soybean growth model. The Tor-Vergata model has been used to test classification schemes [151], to evaluate the potential of radar configurations for applications [152], [153] and to yield insight into radar sensitivity to crop growth [154]–[156].

In the wave approach, both the phase and amplitude of the electromagnetic fields are computed and Maxwell's equations are used to derive the bistatic scattering coefficient. The mean field in the medium can be calculated using the Born approximation (neglects multiple scattering effects) and the renormalization bilocal approximation (accounts for both absorption and scattering). Similar to the energy approach, the models based upon the wave approach (e.g., [157]–[161]) consider horizontally layered random vegetation and the five scattering mechanisms represented in Fig. 2. Unlike the energy approach, the wave approach adds, in amplitude and phase, the scattered field by each vegetation constituent (branches, stems, leaves, etc.), accounting for the orientation and relative position of the constituents. The attenuation and phase shifts within the vegetation are calculated using Foldy's approximation. The total σ^0 is obtained by averaging several realizations of randomly generated vegetation.

Several studies have compared the two approaches. Chauhan *et al.* [162] found σ^0 higher by 3 dB when ground–vegetation–ground interaction was considered for estimating backscatter from corn in mid season at L-band compared to the case when the interaction was ignored. Including the coherent effects produced σ^0 estimates that were closer to observations. Recently, Monsivais-Huertero and Judge [139] founded similar differences between the two approaches during the entire growing season of corn, from bare soil to maturity, at L-band. The coherent effects had a particularly high impact during the reproductive stage of the corn, due to the ears. When each term in (1) was examined closely, it was found that the RT approach predicted σ^0_{veg} as the primary contribution, while the wave approach predicted σ^0_{sv} as the dominant contribution. The HH polarization showed higher differences between the two approaches than the VV polarization, suggesting that the HH polarization is more sensitive to the coherent effects for a corn canopy. The study also indicated that ears were the main contributors during the reproductive stage. Coherent effects were also found to be significant when Stiles and Sarabandi [159], [160] found that the row periodicity of agricultural fields had an impact in the azimuth look angle, particularly at low frequencies such as the L-band.

Energy and wave approaches require moisture content or dielectric properties of the soil and vegetation as well as a description of the size, shape, orientation, and distribution of scatterers in the canopy. This limits their usefulness to the wider, nonexpert community. Despite their complexity, it is important to note that the representing vegetation as a collection of ellipsoids, disks etc., is still a crude simplification of reality. It remains unclear whether such a description is better than more simple, physical models. Nonetheless, they are very useful for relating ground measurements of the parameters during field campaigns to ground-based, airborne, or satellite-based observations and interpreting their respective contributions to backscatter.

C. Polarimetric Decompositions

Polarimetric radar decomposition methods separate total scattering from a target into elementary scattering contributions. This technique can be helpful for establishing vegetation health and for classifying land cover as the dominance and strength of

surface (single bounce), multiple (volume), and double-bounce scattering is largely driven by the roughness and/or structure of the target. More specifically the structure of vegetation varies by type, condition, and phenology state, and as these vegetation states vary so does the mixture and strength of scattering mechanisms. Different polarimetric decomposition approaches allow the polarimetric covariance matrix to be decomposed into contributions assigned to single or odd bounce scattering (indicative of a direct scattering event with the vegetation or ground), double or even bounce scattering (indicative of a scattering event between, for example, a vegetation stalk and the ground) and volume scattering (indicative of multiple scattering events between the ground and vegetation, or among vegetation components) [163], [164]. Yamaguchi [165] introduced a fourth scattering component (helix scattering) to account for copolarization and cross-polarization correlations, as some contributions from double bounce and surface scattering were thought to be contributing to volume scattering [166], [167].

Fig. 3 shows the Freeman–Durden decomposition of three RADARSAT-2 quad-polarization images obtained during SMAPVEX 2012 in Manitoba, Canada. The cropping mix in this region is dominated by spring wheat, canola, corn, and soybeans. In April, producers have yet to plant their crops for the season, so surface and volume scattering from bare soil dominate. In the July image, volume scattering dominates canola (bright green), while wheat fields show considerable double bounce (red).

Cloude and Pottier [168] approached characterization of target scattering by decomposing SAR response into a set of eigenvectors (which characterize the scattering mechanism) and eigenvalues (which estimate the intensity of each mechanism) [169]. Two parameters, the entropy (H) and the anisotropy (A), can be calculated from the eigenvalues . The entropy measures the degree of randomness of the scattering (from 0 to 1); values near zero are typical of single scattering (consider smooth bare soils) while entropy increases in the presence of multiple scattering events (consider a developing crop canopy). Anisotropy estimates the relative importance of the secondary scattering mechanisms. Most natural targets will produce a mixture of mechanisms although typically, one source of scattering dominates. Zero anisotropy indicates two secondary mechanisms of approximately equal proportions; as values approach 1 the second mechanism dominates the third [170]. The Cloude–Pottier decomposition also produces the alpha (α) angle to indicate the dominant scattering source [169]. Single bounce scatters (smooth soils) have alpha angles close to 0°; as crop canopies develop the angle approaches to 45° (volume scattering) although some secondary or tertiary double bounce (nearing 90°) can be observed when canopies include well developed stalks. The Cloud–Pottier decomposition has been employed to retrieve the phenological stage of rice [171] and to identify harvested fields [172].

IV. Applications

The models described in the previous section provide insight into scattering mechanisms, and in particular, into the separation of the contributions from soil and vegetation. The ambiguity between these contributions is one of the main challenges to be addressed in applications of radar observations to agricultural landscapes. The WCM is popular in crop monitoring. Energy and wave approaches have proved very valuable for forward modelling the backscatter from vegetation for soil moisture retrievals, and SAR decomposition methods are most popular in crop classification and monitoring approaches.

A. Regional Vegetation Monitoring Using Spaceborne Scatterometry

Several studies have used the ERS wind scatterometer to determine the fractional cover and seasonal cycles of vegetation. Woodhouse and Hoekman [173] used a mixed target modeling approach to retrieve percentage vegetation cover over the Sahel region and the Hapex Sahel test area from ERS-1 WS data. A subsequent study in the Iberian Peninsula [174] yielded promising results for soil moisture retrieval but revealed that the performance in terms of vegetation cover parameters was site-specific. Frison *et al.* [175] showed that ERS WS data was more effective for monitoring the seasonal variation of herbaceous vegetation in the Sahel compared to SSM/I. The temporal signatures of SSM/I observations were found to depend primarily on air and surface temperature, and integrated water vapor content. Biomass retrievals from SSM/I data were also poor due to the sensitivity of the employed semiempirical model to soil moisture variations. Jarlan *et al.* [176] discussed the difficulty of estimating surface soil moisture and above-ground herbaceous biomass simultaneously without independent *in situ* or remote sensing data to constrain one of the variables. In a subsequent study, soil moisture was estimated using MeteoSat data and a water balance model [177]. This allowed them to map VWC and the herbaceous mass in the Sahelian through the nonlinear inversion of a radiative backscattering model yielding results that were consistent with NDVI observations. Grippa and Woodhouse [178] demonstrated that the inclusion of SAR data and ground measurements to estimate fractional cover in each of four cover classes allowed monthly vegetation properties to be retrieved from ERS WS backscatter at four test sites.

Higher frequency scatterometer data have also been used to monitor vegetation. Frolking *et al.* [40] showed that Ku-band backscatter from the SeaWinds-on-QuikSCAT scatterometer (QSCAT) could be used to monitor canopy phenology and growing season vegetation dynamics at 27 sites across North America. They found good agreement with MODIS LAI, but noted that the onset of growth was often detected earlier in the SeaWinds data than in the MODIS data. Similar results were observed by Lu *et al.* [179] in a comparable study conducted at sites across China. Ringelmann *et al.* [180] identified increases in filtered QSCAT backscatter, associated with improved growing conditions, to estimate the planting dates in a semiarid area in Mali. Hardin and Jackson [181] found seasonal change in backscatter from a savanna area in South America could be attributed due to variations in the dielectric constant of the grass itself accompanied by a strong contribution from soil moisture. Backscatter was found to decrease in the latter part of the

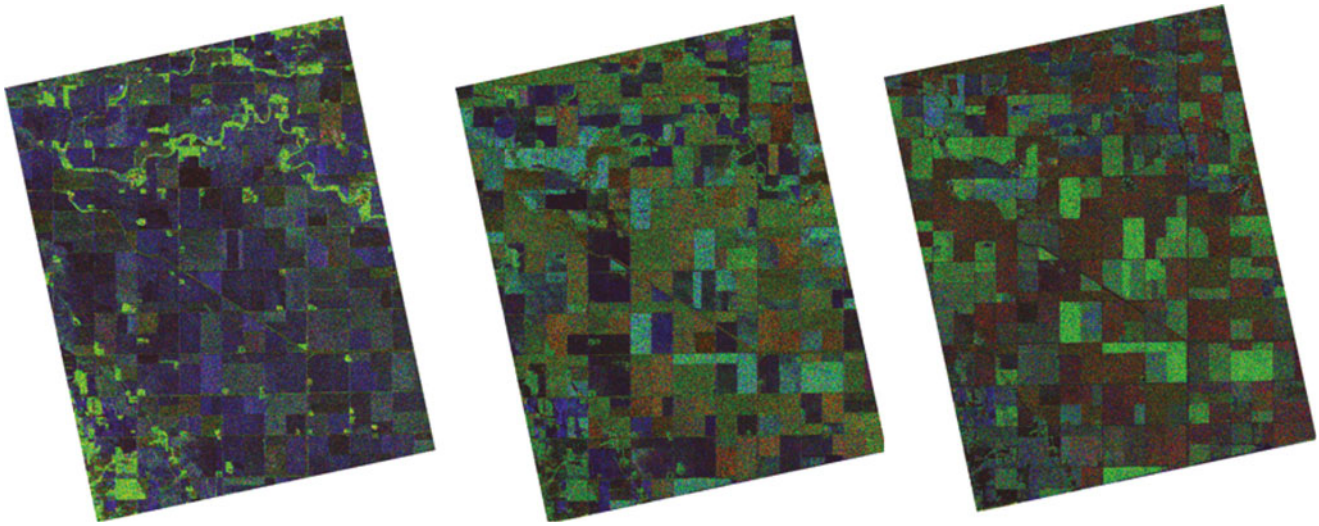

Fig. 3. Freeman–Durden decomposition of RADARSAT-2 quad-polarization data from the 2012 SMAPVEX experiment in Manitoba, Canada. The left image is from April 26, middle from June 13, and right from July 7. Surface scattering is displayed in blue, volume scattering in green, and double bounce in red.

season due to decreasing soil moisture and increased canopy attenuation.

It is important to note that the coarse resolution (typically around 25 km) of the data used in these studies means that they are more suited to regional monitoring than field-scale monitoring. Nonetheless, they demonstrate that scatterometer data are suited for interannual monitoring of the timing and evolution of the growing season, which is useful for regional water resources management, food security monitoring, crop yield forecasting, etc.

B. Crop Classification

The fine resolution of SAR observations make them better suited to field-scale crop classification. The primary advantage cited for integrating SARs with optical data in crop classification strategies is because microwave sensors are unaffected by cloud cover, making SARs a reliable source of data for scientific and operational needs. While this statement is correct, research has proven that optical data are not needed as input to a crop classifier as long as SAR configurations are optimized. As with optical approaches, if a SAR-only solution is to be successful multiple acquisitions through the growing season are needed [37]. At any single point in time two crops (e.g., wheat and oats) can have very similar backscatter. However, as the structure of the crop changes (especially during seed and fruit development), the backscatter changes. Classification can be performed based on these changes, using the variation in backscatter over time to distinguish one crop type from another. The number of images required depends upon the crops present and the complexity of the cropping system (for example, number of crops, consistency of planting practices, presence of intercropping, and number of cropping seasons per year). Le Toan *et al.* [182] showed that the distinctive backscatter changes between two ERS-1 SAR images during a rice growth cycle were enough to identify rice fields. By relating the backscatter to canopy height and biomass, they were also able to map rice fields at different growth stages. A subsequent study by Ribbes [183] found a lower dynamic range in RADARSAT images over rice compared to ERS-1, possibly due to polarization but found that RADARSAT was also potentially useful for rice-mapping. More recently, Bouvet *et al.* [184] used a series of ten X-band images from Cosmo SkyMed to map rice fields in the Mekong Delta, Vietnam. McNairn *et al.* [185] used multiple acquisitions of X-band and/or C-band data to deliver classification results with an overall accuracy of well over 90%, but in a simple corn-soybean-forage cropping system. In fact for this simple system, X-band imagery accurately (90–95%) identified corn only 6 weeks after seeding. However, cropping systems can be much more complex, and in these circumstances, it is important to include later images that capture periods of reproduction and seed development in the classifier, when crop structure changes are most apparent [186], [187].

As stated, successful classification requires multitemporal SAR acquisitions to capture changes in crop phenology. When considering the SAR configuration, choice of frequency is very important. This choice is not straightforward and the canopy (in terms of crop type and development) must be considered. Enough penetration is needed for microwaves to scatter into the canopy but when frequencies are too low, too much interaction occurs with the soil.

Inoue *et al.* [62] showed that, for rice, X- and K-band backscatter were sensitive to thin rice seedlings but poorly correlated with biomass and LAI, which were better correlated with L- and C- band, respectively. Data from several spaceborne SARs including ERS 1/2 SAR, Envisat ASAR, Radarsat and Advanced Land Observing Sate (ALOS) PALSAR have been used to map rice growth [182], [183], [188]–[190]. Jia *et al.* [191] favored longer wavelengths at C-Band over X-Band for separating winter wheat from cotton. McNairn *et al.* [186] found that longer L-Band data were needed to accurately identify higher biomass crops (corn, soybean), although C-Band data were most suit-

able for separating lower biomass crops (wheat, hay pasture). Because cropping systems include wide ranges of crops with varying volumes of biomass, researchers have consistently advocated for an integration of data at multiple frequencies to ensure high accuracy crop maps. Increases in accuracies have been reported when X- and C-Band data were integrated [191], C- and L-Band [186], [192], [193], X-, C-, and L-Band [35] as well as C-, L-, and P-Band [194]–[198]. The largest gains in accuracy are often observed for individual crop classes. In McNairn *et al.* [185], accuracies for individual crops increased up to 5% (end of season maps) and 37% (early season maps) when both X- and C-band were used together.

By and large, radar parameters that are responding to multiple or volume scattering within the crop canopy are the best choice for crop identification. Many studies have confirmed that the cross polarization (HV or VH) is the single most important polarization to identify the majority of crops [63], [102], [186], [199]–[201]. The greatest incremental increase in accuracy is then observed when a second polarization is added to the classifier [102], [199], [200]. Agriculture and Agri-Food Canada, for example, integrates C-Band dual-polarization SAR (VV and VH from RADARSAT-2) with available optical data for their annual crop inventory [202]. This inventory is national in scale and is run operationally, delivering annual crop maps with overall accuracies consistently at or about 85%. Although the greatest improvements are observed when adding a second polarization when available, a third (such as HH) can increase accuracies for some crops [102], [186], [203].

Limited research has been published on the use of scattering decompositions within the context of crop classification. What has been presented has indicated small yet important incremental increases in accuracies. At L-Band, McNairn *et al.* [186] demonstrated that overall accuracies improved up to 7% when decomposition parameters (Cloude-Pottier, Freeman-Durden) were used instead of the four linear intensity channels (HH, VV, VH, HV). Differences in the relative contributions of scattering mechanisms among the crops were observed leading to improved classification. Liu *et al.* [163] used RADARSAT-2 data and the three Pauli components in a maximum likelihood classifier, applying this to a relatively simple cropping mix (corn, wheat, soybeans, hay pasture). Two test years established an overall accuracy of 84–85%, using only these C-band data. Compact polarimetric (CP) data (in circular transmit-linear receive configuration) has been simulated from RADARSAT-2 C-band data and also assessed for crop classification. Using the Stokes vector parameters from synthesized CP data (four images through the season) classification accuracies of 91% were reported with individual crop classification accuracies ranging from 81–96% (corn, soybeans, wheat, and hay pasture) [204].

C. Crop Monitoring

Global, national, and regional monitoring of crop production is critical for a host of clients. These clients include those concerned with food security where foresight into production estimates are needed to address potential food shortages, commodity brokers looking for information to facilitate financial decision making and agri-businesses, which can more effectively deploy harvesting and transportation resources if production estimates are known in advance. Forecasting production is not a trivial task and as described in Chipanshi *et al.* [205] methods can be categorized as statistical, mechanistic, or functional, with Earth observation data increasingly being used as data input into crop condition, production and yield forecasting. Agronomists are often interested in exploiting LAI or biomass as surrogates, since both are good indicators of potential crop yield [206]. The structure of a crop canopy significantly impacts the intensity of scattering, type of scattering and phase characteristics. This structure is crop specific and varies as crop phenology changes. As such, research as far back as 1984 [207] and 1986 [208] has demonstrated a strong correlation between backscatter intensity and LAI. These researchers focused on higher frequency K- and Ku-band and noted strong correlations with the LAI of corn; weaker correlations being reported for wheat. This early research encouraged additional study into the sensitivity of SAR to LAI, leading to findings of strong correlations between C-band backscatter and LAI for wheat [209], corn and soybeans [210], and cotton [211]. Prasad [212] reported strong correlations between X-band backscatter and soybeans; Kim *et al.* [213] using L-, C-, and X-band backscatter for soybeans. Liu *et al.* [163] examined RADARSAT-2 data to track LAI development of corn and soybeans using Pauli decomposition parameters. Wiseman *et al.* [214] observed strong correlations between C-band responses and the dry biomass of corn, soybeans, wheat, and canola. Much of the earliest research focused on linear like-polarized responses (for example, Ulaby *et al.* [207] and Paris [208] examined HH and VV polarizations). Scattering from crop canopies is a result of multiple scattering from within the crop canopy, and between the canopy and soil. As such, repeatedly the highest correlations with LAI and biomass have been found for SAR parameters indicative of these multiple scattering events. These parameters include HV or VH backscatter, pedestal height, and volume scattering components from decompositions and entropy ([195], [196], [209], [210], [214]–[216] all using C-band). Although SAR parameters responsive to volume scattering have proven most sensitive to crop condition indicators such as LAI and biomass, a few researchers have reported success in combining polarizations in the form of ratios. This has included a C-band HH/VV ratio for wheat biomass [21], wheat LAI [217], and rice LAI [218]. C-HV/HH proved sensitive to the LAI of sugarcane [219].

In 2009, Kim and van Zyl [220] introduced the RVI, whereby RVI is expected to increase (from 0 to 1) as volume scattering increases due to canopy development. RVI is defined as

$$\mathrm{RVI} = \frac{8\sigma^0_{\mathrm{hv}}}{\sigma^0_{\mathrm{hh}} + 2\sigma^0_{\mathrm{hv}} + \sigma^0_{\mathrm{vv}}} \tag{6}$$

where σ_0 is SAR intensity for each transmit (h or v) and receive (h or v) polarization.

Fig. 4 shows a time series of RVI calculated from data collected during Microwex 10 with the UF-LARS. Though HV is typically lower than copolarized backscatter, it is clearly most sensitive to the increasing biomass, indicated by increasing LAI. RVI is less than 0.2 up to 30 days from planting be-

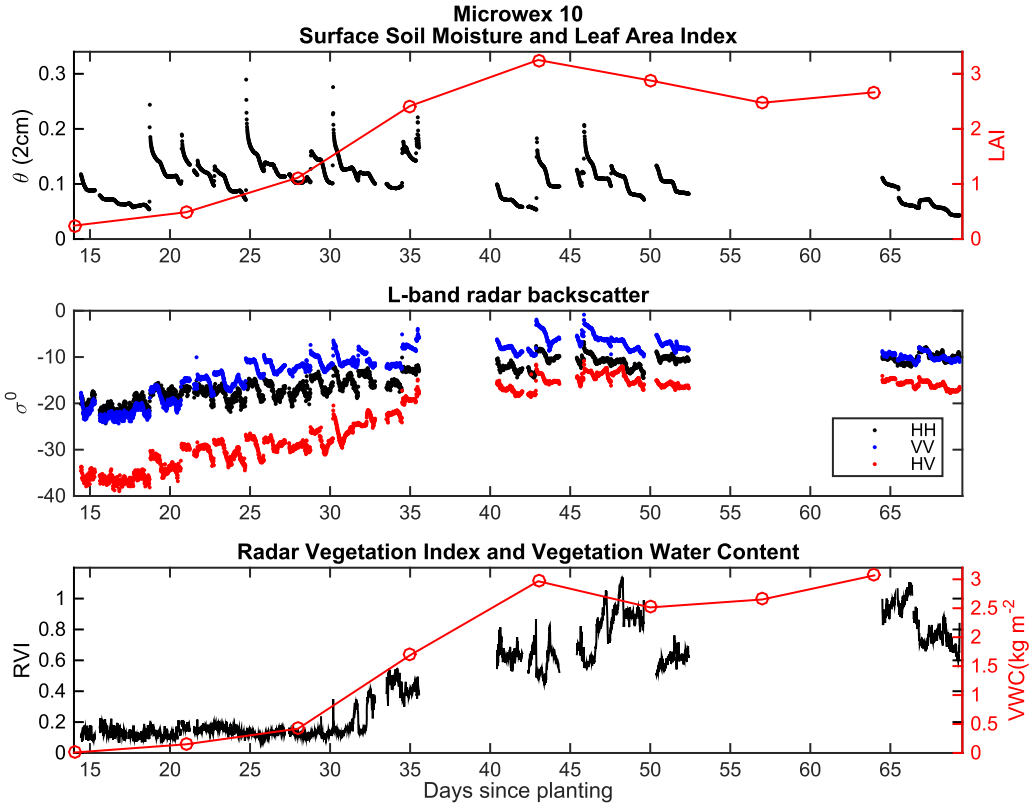

Fig. 4. Data collected in a corn canopy during Microwex10. Top: Surface (2.5 cm) soil moisture, and LAI. Middle: Co- and cross-polarized backscatter σ^0. Bottom: RVI and VWC.

cause the magnitude of HV is much lower than the copolarized backscatter. After this date, RVI increases steadily until the plant reaches full growth. Fluctuations in RVI reflect changes in soil moisture (influencing co-pol backscatter), and VWC (influencing cross-pol backscatter). RVI has been statistically correlated with the plant area and biomass of some crops [214], [221], [222]. It has also been used to estimate VWC for soil moisture studies, e.g., [223] and [224].

Radar response from crop canopies can saturate at higher LAI or biomass. This means that as the crop continues to accumulate plant matter, the radar backscatter is no longer responsive to these increases. The exact point of saturation is crop and frequency specific. For corn, McNairn *et al.* [102] founded that C-HH saturated at a height of one meter. When considering LAI, saturation has been reported at LAI of 2-3 (Ulaby *et al.*, [207], using K-band), LAI of 3 for corn and soybeans [210], and LAI of 3 for rice [135]. Not all research has reported saturation; For winter wheat, backscatter continued to be sensitive to crop development throughout the season [96]. Although saturation is problematic when monitoring some crops during the entire season, a critical window for crop yield forecasting is during the period of rapid crop development up until peak biomass accumulation. Wiseman *et al.* [214] reported exponential increases in C-band responses in the early season when biomass accumulation accelerated, especially for parameters such as entropy (corn and canola) and HV backscatter (soybeans). Thus, SAR-based estimates of LAI, even if restricted to periods prior to peak biomass accumulation, will be useful in monitoring crop productivity. These studies which reported a sensitivity of SAR to LAI and biomass gave rise to efforts to model and eventually estimate biophysical parameters indicative of crop condition. The WCM has been a choice approach to estimate crop parameters given its relative simplicity to model and invert. The influence of soil moisture on SAR response dissipates as the canopy develops. Prevot *et al.* [96] reported that at X-band once the LAI of wheat reached four, soil contributions were negligible. At C-band, once the LAI of corn and soybeans reached three, 90% of scattering originates from the canopy [210]. Nevertheless, considering the requirement to model the entire growth cycle, it remains important to consider soil moisture contributions within the WCM. Ulaby *et al.* [207] demonstrated that when LAI is less than 0.5, backscatter is dominated by soil moisture contributions. One approach to LAI retrieval with the WCM is to provide ancillary sources of soil moisture. This is particularly effective when the number of available SAR parameters is not sufficient to retrieve multiple unknown variables modeled by the WCM. This approach was demonstrated by Beriaux *et al.* [137]. Here, VV backscatter was used to estimate the LAI of corn, using ancillary sources of soil moisture. LAI errors (RMSE in m^2/m^2) were reported as 0.69 (using soil moisture from ground penetrating radar), 0.88 (using field measurements) and 0.9–0.97 (using moisture modeled by SWAP). If multiple SAR parameters are available, LAI can be retrieved without provision of ancillary soil moisture data. Prevot *et al.* [96] did so using two

frequencies (X-band and C-band) and reported an RSME for retrieval of LAI for winter wheat as 0.64 m^2/m^2. Soil moisture was also retrieved (RSME of 0.065 cm^3/cm^3). In a slightly modified approach, Hosseini *et al.* [136] used multiple polarizations from RADARSAT-2 and an airborne L-band sensor to invert the WCM without the need for ancillary moisture data. In this case, LAI was accurately estimated using C-VV and C-VH backscatter for corn (RMSE of 0.75 m^2/m^2) and soybeans (RMSE of 0.63 m_2/m_2). Errors using L-band were at or above RMSE of 1, perhaps indicating too much penetration for accurate LAI retrieval for these canopies. Research continues in this domain, yet it is evident that SAR can provide estimates on LAI to support the monitoring of crop condition. In fact, error statistics for retrieval of LAI for corn and soybeans using RADARSAT-2 [136] were slightly lower than those achieved using optical RapidEye data [225], both experiments occuring in Canadian cropping systems.

Beyond LAI, polarimetric SAR (PolSAR) has proved very valuable for monitoring phenological stages of rice [226]–[231] and other crops [221], [232]–[234]. Recently, Vicente-Guijalba *et al.* [235] presented a dynamic approach for agricultural crop monitoring. First, a dynamical model for crop phenological change is extracted from a reference dataset (e.g., a stack of SAR images). Then, this model is constrained by input data using an extended Kalman filter to estimate the crop phenological stage on a continuous scale in real time. They demonstrated using Radarsat data from AgriSAR2009 that the approach worked well for wheat and barley. For oats, the sensitivity was only sufficient in the first and last stages. In related studies, data fusion [236] and data assimilation [237], [238] techniques were also successfully used to extract key dates or phenological stages from stacks of SAR images. Mascolo *et al.* [239] presented a novel methodology that uses distances among covariance matrices derived from series of PolSAR images to identify both the phenological intervals to be estimated. It also determines the training sets for each interval and the intervals are then classified by the complex Wishart classifier. The advantage is that this method obviates the need to identify specific PolSAR features. They demonstrated, using RADARSAT-2 data from the AgriSAR2009 campaign, that this methodology can be used to retrieve the phenological stages of four different crop types namely oat, barley, wheat, and corn. Finally, PolSAR interferometry, in which the strengths of interferometry are combined with those of PolSAR, has been put forward to address some of the shortcomings of PolSAR in agricultural monitoring [240]. PolInSAR yields information about the localization of the scattering centers, and hence the vertical structure of the plant. Lopez-Sanchez and Ballester-Berman [240] argue that this may be used to overcome the saturation effects observed in PolSAR and to monitor plant phenological stage.

D. Soil Moisture

Soil moisture is important in its own right for agricultural scheduling and water resources management [241] and drought monitoring [242]. Furthermore, soil moisture observations can be used to account for the influence of drought conditions on crop yield forecasts [243]–[245]. The soil moisture dataset derived from the ERS 1/2 wind scatterometers and the ASCAT, provides one of the longest-duration global records of soil moisture and is the only operational global soil moisture product derived from radar observations [246]. It is based on an empirical soil moisture retrieval algorithm that accounts for seasonality in the influence of vegetation on the sensitivity of backscatter to soil moisture [247]. First, the entire record of backscatter coefficients from the ERS wind scatterometer is extrapolated to a reference angle of 40°, yielding a time series $\sigma^0(40,t)$. The highest and lowest values of $\sigma^0(40,t)$ for each grid cell, $\sigma^0_{\text{wet}}(40,t)$ and $\sigma^0_{\text{dry}}(40,t)$, are identified. The first is generally independent of vegetation status, while $\sigma^0_{\text{dry}}(40,t)$ varies seasonally with vegetation phenology. Assuming that $\sigma^0(40)$ and the surface soil moisture are linearly related, the relative moisture content of the surface (0.5–2-cm thick) layer is given by

$$m_s(t) = \frac{\sigma^0(40,t) - \sigma^0_{\text{dry}}(40,t)}{\sigma^0_{\text{wet}}(40,t) - \sigma^0_{\text{dry}}(40,t)}. \tag{7}$$

This approach was developed for a study in the Iberian peninsula [247]. In a subsequent study, the approach was validated using an extensive *in situ* dataset from Ukraine [248] and a soil water index (SWI) was introduced to provide a measure of profile soil moisture. SWI is obtained as a convolution of the time series of surface moisture content with an exponential filter function such that

$$\text{SWI}(t) = \frac{\sum_i m_s(t_i) e^{-(t-t_i)/T}}{\sum_i e^{-(t-t_i)/T}} \tag{8}$$

for $t_i \leq t$, where m_s is the surface soil moisture from the ERS WS at time t_i, T is some characteristic time length between 15 and 30 days. Wagner *et al.* [249] evaluated both products over West Africa. They demonstrated that the temporal and spatial distributions of the estimated m_s and SWI captured the influence of the wet and dry seasons and that the estimated slope parameters were consistent with the distribution of land cover. Wagner *et al.* [250] presented first global, multiannual soil moisture data set (1992–2000) from satellite remote sensing. Due to the lack of a global network of *in situ* validation data, the estimated soil moisture was compared with observed monthly precipitation data, and monthly soil moisture obtained from a dynamic global vegetation model. A comparison of anomalies in SWI and precipitation anomalies yielded correlations up to 0.9 in tropical and temperature regions. Though spurious effects were observed in steppe and desert climates, this study illustrated the potential value of spaceborne scatterometer data for soil moisture estimation. Following the launch of the first of three METOP satellites in October 2006, Bartalis *et al.* [251] used the parameters derived from eight years of ERS scatterometer data, to produce first global soil moisture maps from the METOP-A ASCAT commissioning data. Comparison of the ASCAT-derived surface soil moisture to rainfall and NDVI data suggested that the approach developed for the ERS scatterometer could be applied to ASCAT data with minimal adaptations required to the processing chain and configuration.

Naemi *et al.* [252] made several improvements to address shortcomings in the original algorithm to yield the so-called WARP5 model.

Soil moisture estimates derived from both the ERS WS and MetOp ASCAT, using a newer WARP5.2 are key components of the European Space Agency Climate Change Initiative (ESA CCI) soil moisture product [253]. A recent study by Vreugdenhil *et al.* [254] highlighted the need to better account for the influence of vegetation dynamics on soil moisture retrieval, particularly in areas where there is significant interannual variability in vegetation.

NASA's SMAP mission was launched on January 31, 2015 with an L-band radiometer and L-band SAR on board. The SMAP baseline algorithm for the radar-only soil moisture product was to use a multichannel datacube retrieval approach outlined by Kim *et al.* [255], [256]. Forward backscatter models for 16 vegetation classes and bare soil are used to simulate backscatter as a function of the real part of the soil dielectric constant (ϵ_r), roughness (s), and VWC. Scattering from each of the vegetation types is simulated using the methods described in Section III-B, and based on data collected from field campaigns. For retrieval σ_{HV} or ancillary data is used to determine VWC and a time series of copolarized backscatter is used to determine a single value for s and a time series of ϵ_r by minimizing the difference between simulated and observed backscatter [6]. In addition to this baseline algorithm, the change detection approaches of van Zyl and Kim [257] and Wagner *et al.* [247] are considered as optional algorithms. Unfortunately, the failure of the radar in July 2015 means that SMAP products are currently limited to those from the radiometer alone.

V. Challenges and Opportunities

A. Resolution of Spaceborne Scatterometry Data

The coarse resolution of spaceborne scatterometer observations remains a challenge. However, resolution enhancement [258], [259], data assimilation [260]–[262], and downscaling approaches [263] offer new possibilities in terms of extracting field-scale or, at least, finer-scale information from coarse scatterometer observations for agricultural applications.

B. Limitations of Operational SAR Applications

Spatial and temporal coverage remains a huge challenge for operational SAR applications in agriculture. The results discussed here illustrate that theoretically, radar data are an excellent option for crop type monitoring to support production estimates, and to monitor crop condition. The quality of multifrequency radar data retrievals in these applications is sufficiently high to obviate the need for optical data. The recent launches of Cosmo Sky-Med (4 day revisit time) and Sentinel 1a and 1b (6 day revisit time) have greatly improved temporal coverage. Nonetheless, spatial and temporal availability of data remains a barrier to operational global, regional, or even national monitoring. For example, the current state-of-the-art operational monitoring performed by Agriculture and AgriFood Canada still relies on the integration of radar and optical data.

Furthermore, to transition from scientific applications to operational monitoring, the current model (i.e., WCM) needs to be adapted so that it can be applied for a wider range of cropping systems. Finally, the extensive history of using optical data in agriculture means that users are familiar with the processing and interpretation of optical imagery. The complexity of SAR scattering means that applications specialists in agricultural monitoring generally consider interpretation of radar images more difficult than optical images. This is a major barrier to the widespread adoption of radar for operational monitoring, most of which is carried out by national institutions. User community participation and capacity-building activities are needed to ensure that radar products are provided to users in a format that they can readily use.

C. Water Stress Monitoring Using Spaceborne Radar

An emerging topic of research is the potential use of diurnal variations in backscatter to identify the onset of water stress. Friesen [264] identified statistically significant diurnal differences in backscatter from the ERS 1/2 wind scatterometer over West Africa. A hydrological model, and a degree-day model were used to demonstrate that the largest differences coincided spatially and temporally with the onset of water stress [264]. A sensitivity study using the MIMICS model showed that the variations may be attributed to variations in the water content (and hence, relative permittivity) of the leaves and trunks [265]. The challenge remains to disentangle the artifacts of WS preprocessing from the influence of variations in dielectric properties and geometric changes in the canopy due to the forest's physiological response to water stress. Diurnal variations have been detected in higher frequency spaceborne observations too [3], [266]–[268]. Frolking *et al.* [2] identified a decrease in backscatter over the southwestern Amazon forest during the 2005 drought. The most significant anomalies, with respect to interannual variability, were in the morning backscatter anomalies. Strong spatial correlation with water deficit anomalies suggested that these anomalies were due to drought—hypothesizing, similarly to Friesen [264], that the changes were due to changes in water relations within the tree in response to stress.

In the agricultural context, diurnal differences in backscatter were also observed in agricultural canopies in tower-based measurements as early as the 1970s [64], [269], and were attributed to loss of canopy moisture during the day due to transpiration. A more recent study in an agricultural maize canopy found diurnal changes in bulk VWC up to 30% and leaf VWC up to 40% during a period of water stress [28]. WCM simulations were used to illustrate that the variations in leaf VWC had a significant impact on total backscatter, particularly at C-band and higher frequencies. Schroeder *et al.* [270] normalized ASCAT backscatter to 54° to maximize sensitivity to the slope factor. Recall from Wagner *et al.* [247] that the slope factor reflects variations in VWC or phenology. Schroeder *et al.* founded that negative anomalies in $\sigma^0(54)$, particularly during the morning overpasses, were spatially and temporally consistent with the drought patterns observed in 2011 and 2012 by the U.S. Drought Monitor. Additional research is needed to relate the observed backscatter

variations with the underlying plant response to drought, and hence to explore the potential of scatterometer and SAR data at different frequencies to identify water stress at regional and field scales, respectively.

D. New Opportunities With ASCAT

Twenty five years since the launch of the Active Microwave Instrument on ERS-1, sensors that were primarily launched for ocean applications are at the core of operational remote sensing for land surface monitoring. The continuation of ASCAT on MetOp will provide essential operational soil moisture data for the meteorological, hydrological, and land monitoring communities [271]. Recent research by Vreugdenhil [254] demonstrates that there is valuable information about vegetation dynamics in the ASCAT observations. The ability to quantitatively exploit this information could lead to improved soil moisture retrieval and vegetation phenology monitoring.

E. Vegetation Dynamics From RapidScat on ISS

Paget and Long [3] recently mapped diurnal variations in Ku-band backscatter observations from RapidScat. Significant variations were observed across several vegetation biomes. Though previous studies have indicated that diurnal variations at several frequencies could be due to variations in water dynamics [264], [272], [273], uncertainty still surrounds the relationship between plant water relations, variations in dielectric properties, and the observed backscatter [2], [3], [265], [274]. Understanding what drives these diurnal backscatter variations is the first step to exploiting RapidScat for agricultural applications. Furthermore, their exploitation would also yield valuable insight into the potential value of the ISS as a platform for vegetation monitoring using radar.

F. New C-band SAR Missions

Two new C-band SAR constellations offer global high-resolution imagery at an unprecedented spatial and temporal resolution, thereby, offering the potential to more accurately pinpoint growth stages and monitor biomass accumulation, VWC, etc. The two satellites of ESA's C-band Sentinel-1 Mission were launched in 2014 and 2015, respectively. These are the first in a series of operational satellites in the frame of ESA's Global Monitoring for Environment and Security Space Component programme. The two satellites are in the same orbital plane providing an average revisit time of two days above 45° N/S and global exact repeat coverage every two weeks. It has four imagine modes: the interferometric wide-swath model, wave mode (WM), strip map mode, or extra-wide swath model. Apart from the single-polarization WM, all modes have dual polarization with VV and VH as the default [275]. Canada's three-satellite RADARSAT Constellation Mission (RCM) is scheduled for launch in 2018. It will support the operational requirements of the Government of Canada and to provide data continuity for existing users of RADARSAT-1 and RADARSAT-2 [276]. RCM will have a range of modes from wide area surveillance modes (500-km swath) to spotlight modes (5-km swath). Single or dual polarization acquisitions (HH + HV or VV + VH or HH + VV) are possible for each mode. The constellation also provides access to both quad-polarization and compact polarization (CP) modes. RCM will have a 12-day repeat cycle and with three satellites, 4-day coherent change detection will be possible. From Section IV, it is clear that the exploitation of SAR data, particularly Radarsat1 and Radarsat 2 data, has significantly contributed to our understanding of scattering mechanisms in vegetation. Similarly, knowledge generated from the use of Sentinel-1 and RCM can be transferred to improve our understanding of scatterometry and facilitate increase exploitation of the data collected by ASCAT on MetOp and other spaceborne scatterometry missions.

G. Combined SMAP/Sentinel-1 Soil Moisture

One of the objectives of NASA's SMAP mission was to combine the radiometer and radar observations to produce a merged soil moisture product at 9-km resolution. Sentinel-1 observations have been proposed as a potential substitute for SMAP radar observations in this combined product since the radar failure in July 2015 [277]. However, there are several differences between the SMAP radar data and the Sentinel-1 SAR data that will need to be addressed. In addition to the difference in frequency between the two radars, and the incidence angle diversity of Sentinel-1, the main challenge is that the two instruments are not in the same orbit. Any downscaling approach must, therefore, be robust enough to merge acquisitions from the SMAP radiometer and Sentinel-1 radar that are separated by hours or even days. Combined multiangle, C- and L-band radar observations from tower-based scatterometers could play an important role in developing and validating proposed downscaling approaches to take these differences into account.

H. Scattering Models for Vegetation

The persistent dilemma in terms of radar applications for vegetation is choosing an appropriate model. The WCM remains widely used despite, if not because, of its simplicity. However, its key assumptions regarding the distribution of moisture in the canopy are generally not valid. The more theoretical energy and wave-based approaches remain primarily in the research domain due to the large number of input parameters required (e.g., dielectric properties of soil and vegetation, geometry, etc.). This data collection requirement may be possible during intensive field campaigns, but it is too time consuming and expensive to be performed regularly and for all possible vegetation cover types. Furthermore, the representations of the canopy in energy and wave-based models are still simplifications of reality. For emerging applications, it is significant that the relationship between these parameters and vegetation (particularly water) dynamics is currently not well understood. A new approach to modeling is needed that reflects the known non-uniformity and dynamic profile in moisture content, and the importance of multiple-bounce between the soil surface and overlying vegetation. However, to ensure that the model is universally applicable, it needs to be as simple to parameterize and use as the WCM.

I. Radar Tomography

From the discussions in the previous sections, it becomes clear that the main limitation of conventional single- or quad-polarimetric acquisitions, arises from the fact that they do not provide the required dimensionality to resolve unambiguously the multiple and/or complex scattering processes ongoing at different polarizations and frequencies. A potential solution to this are multi-angular acquisitions that allow the reconstruction of the 3-D reflectivity of volume scatterers by means of tomographic techniques. In the context of agricultural crops, the first experiments and demonstrations where performed by means of ground-based scatterometers in indoor and outdoor set-ups [278]. More recently, the developments in SAR technology and data processing allowed first tomographic airborne SAR experiments over agricultural fields even at higher frequencies [279], [280].

Airborne tomographic SAR experiments are mostly carried out by displacing the multiple acquisitions on a linear configuration such that the variation of the radar look angle amounts to a small fraction of a degree between consecutive acquisitions [281]. In conventional linear tomography the 3-D reflectivity is inverted from the multiacquisition data vector by means of a Fourier-based approach [281], [282]. In this case, the spatial resolution in the elevation direction (also referred to as cross-range direction, i.e., the direction perpendicular to the radar LoS) is defined by the length of the formed synthetic aperture L_X, that corresponds to the maximum separation (in elevation) between the acquisitions as

$$\delta = \frac{\lambda}{2L_X} r_0 \tag{9}$$

where λ is the radar wavelength and r_0 the distance between radar and scatterer. For example, in order to achieve, with an X-band radar, a resolution in elevation of 1 m at a distance $r_0 = 5$ km, an aperture of 150 m is required. While the maximum separation between the acquisitions is defined by the resolution requirement, the number of acquisitions needed for tomographic imaging is given by the distance between the acquisitions required to fulfil Nyquist sampling. For a scatterer (e.g., agricultural field) with height H_X in elevation, the minimum required distance between the acquisitions is given by [281]

$$d_X = \frac{\lambda}{2H_X} r_0. \tag{10}$$

Equations (9) and (10) make it clear that the lower heights of agricultural vegetation require high vertical resolutions and demand a larger number of acquisitions. In the example used previously for mapping a $H_X = 3$-m tall agriculture field, a minimum distance of 25 m between the acquisitions is required so that in total seven acquisitions are at least required assuming a uniform spacing among them.

For each SAR image pixel, the reflectivity profile can be inverted from the related multiacquisition data vector by means of a Fourier-based approach [281], [282]. However, the reconstructed profile will in general be affected by the presence of sidelobes that can lead to misinterpretations of the reflectivity distribution. On the other hand, a resolution better than the one provided by the tomographic aperture [see (9)] is desired, especially for small vegetation volumes like crops. In order to improve the reconstruction performance and to relax the acquisition requirements, adaptive reconstruction algorithms have been proposed. One interesting and popular example is the Capon spectral estimator, a widely employed low-complexity solution [282]. More recently, compressive sensing reconstruction techniques that allow a high-performance reconstruction even with a very low number of acquisitions (that may even not fulfil the Nyquist sampling condition) have been proposed [283]. Both algorithms have been demonstrated to greatly improve the reconstruction of the reflectivity profile in terms of side-lobe cancellation and resolution enhancement, at the cost of some (generally acceptable) radiometric nonlinearity.

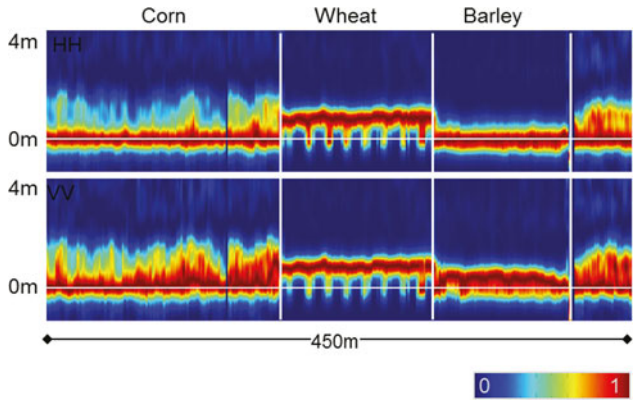

Fig. 5. Normalized tomographic reflectivity profile across three fields (corn, wheat, and barley) at X-band with a vertical resolution of $\delta_Z = 0.5$ m at HH (top) and VV (bottom).

Fig. 5 shows a Capon tomographic reflectivity profile across three fields (corn with a physical height of 1.8 m at the time of the acquisition, wheat with a height of 0.8 m, and barley with a height of 0.8 m) at X-band with a vertical resolution of 0.5 m formed by nine airborne SAR acquisitions performed on the 3rd of July 2014 over the Wallerfing test site (South Germany). Looking at the profile, one can clearly distinguish the different scattering processes. The corn field, which is still in its early development stage, is dominated by dihedral scattering (by HH dominated scattering located on the ground). Over the wheat field, surface scattering on the top layer is ongoing and the row spacing is clearly visible. Over the dry barley field, the vegetation at HH is almost "invisible" and only appears weakly in VV [280].

Fig. 5 illustrates that tomographic imaging has the potential to make a critical and unique contribution to our understanding of scattering from agricultural scenes as it allows us to identify the dominant scattering processes as well as their change in time at different polarizations and frequencies. This is essential for understanding propagation and scattering within agriculture vegetation and interpreting correctly conventional back-scattering signatures. The availability of multitemporal tomographic acquisitions is especially critical when it comes to determine processes that effect the dielectric and/or geometric characteristics of the scatterers.

However, the large number of acquisitions, combined with the fast temporal evolution of agricultural plants, limits the application of radar tomography to rather small-scale ground-based and/or airborne experiments. Spaceborne repeat-pass implementations are limited by temporal decorrelation that has more of an effect on the higher frequency range preferred for agricultural vegetation applications. An interesting alternative—proposed and used for forest tomography—are single-pass spaceborne configurations that are able to provide tomographic imaging based on (single pass) interferograms acquired at consecutive repeat-pass cycles [282]. However the fast development of agriculture plants requires very short repeat-pass cycles in order to avoid changes in the 3-D-reflectivity due to the plant evolution. Accordingly, until the next generation of multistatic spaceborne SAR configurations becomes operational, the availability and coverage of tomographic data will be limited but significant for the development of simplified inversion approaches invertible with a "slimmer" in terms acquisitions observation space [240], [284]–[287] .

J. Innovative Ground Measurements

Several innovative ground measurement techniques offer new insight into vegetation dynamics, specifically biomass accumulation and VWC variations, i.e., GPS-IR [288]–[290], wireless networks [291], and COSMOS [292], [293]. These ground-based sensors yield indirect, though continuous estimates of VWC and biomass which could fill the gaps between less frequent destructive sampling. Data from these new sensors with conventional measurements of plant architecture and moisture profile could be combined with continuous tower-based scatterometry to study subdaily variations in backscatter and to develop new models that account for variations at scales not considered in the current formulation of the WCM.

VI. Conclusion

Ground-based and aircraft-based experiments have been central to our understanding of backscatter from vegetation and how it depends on system parameters (frequency, polarization, incidence, and azimuth angle) and surface characteristics (soil moisture and roughness, vegetation moisture, and geometry). They have also played a crucial role in the development and validation of models and decomposition methods. This has enabled the development of radar as a tool for agricultural applications, particularly crop classification, crop growth monitoring, and soil moisture monitoring.

Though spaceborne scatterometry has been used to monitor vegetation phenology at regional scales, field scale classification and crop monitoring has primarily exploited spaceborne SAR due to its fine resolution. Limited coverage, until now, has hindered widespread operational use. The rather long revisit time of SAR missions to date has limited their use for soil moisture monitoring. Despite their coarse resolution, soil moisture products from the ERS 1/2 wind scatterometer and ASCAT on MetOp have become a data cornerstone in hydrological and climate studies. Recent advances in both SAR and scatterometry demand improved representation of vegetation dynamics.

The recent launch of the Sentinel-1 satellites and the upcoming Radarsat Constellation mean that C-band SAR observations will be available with unprecedented revisit time opening the possibility of observing vegetation dynamics at a finer temporal scale than ever before. At the same time, several studies using spaceborne scatterometry data (C-band and K-band) have revealed that backscatter is sensitive to VWC variations and in particular to water stress. These developments demand the ability to understand and simulate scattering from vegetation at finer temporal scales than ever before.

To ensure that we can exploit both SAR and scatterometry data to its full potential, we need to develop models that consider vegetation as a dynamic scattering medium rather than a medium that changes slowly over the growing season. Being able to quantify the influence of water dynamics on backscatter could lead to improved soil moisture retrievals, and reduce uncertainty in crop classification and monitoring applications. It would also stimulate the development of regional scale water stress monitoring based on spaceborne scatterometry. Innovative methods like GPS-IR and radar tomography can play a vital role in characterizing the dynamics of the moisture distribution. Coupling these with ground-based scatterometry experiments would provide a detailed and rich dataset with which to revisit the modeling of backscatter of vegetation. Improvements in current applications and the development of emerging applications will facilitate the exploitation of the new generation of SAR satellites, and the continued exploitation of the historic and operational data record from spaceborne scatterometry.

References

[1] J. Friesen, S. C. Steele-Dunne, and N. van de Giesen, "Diurnal differences in global ERS scatterometer backscatter observations of the land surface," *IEEE Trans. Geosci. Remote Sens.*, vol. 50, no. 7, pp. 2595–2602, Jul. 2012.

[2] S. Frolking, T. Milliman, M. Palace, D. Wisser, R. Lammers, and M. Fahnestock, "Tropical forest backscatter anomaly evident in SeaWinds scatterometer morning overpass data during 2005 drought in Amazonia," *Remote Sens. Environ.*, vol. 115, no. 3, pp. 897–907, Mar. 2011.

[3] A. C. Paget, D. G. Long, and N. M. Madsen, "RapidScat diurnal cycles over land," *IEEE Trans. Geosci. Remote Sens.*, vol. 54, no. 6, pp. 3336–3344, Jun. 2016.

[4] F. Ulaby, R. More, and A. Fung, *Microwave Remote Sensing: Active and Passive. Vol. I: Microwave Remote Sensing Fundamentals and Radiometry*. Boston, MA, USA: Artech House, 1986.

[5] F. Ulaby, P. Dubois, and J. van Zyl, "Radar mapping of surface soil moisture," *J. Hydrol.*, vol. 184, no. 1-2, pp. 57–84, Oct. 1996.

[6] S.-B. Kim *et al.*, "SMAP L2 & L3 Radar Soil Moisture (Active) Data Products," 2012. [Online]. Available: https://media.asf.alaska.edu/uploads/l2%263_sm_a_initrel_v1_5.pdf

[7] F. Ulaby, "Radar response to vegetation," *IEEE Trans. Antennas Propag.*, vol. 23, no. 1, pp. 36–45, Jan. 1975.

[8] F. Ulaby, T. Bush, and P. Batlivala, "Radar response to vegetation II: 8-18 GHz band," *IEEE Trans. Antennas Propag.*, vol. 23, no. 5, pp. 608–618, Sep. 1975.

[9] A. Joseph, R. van der Velde, P. O'Neill, R. Lang, and T. Gish, "Effects of corn on C- and L-band radar backscatter: A correction method for soil moisture retrieval," *Remote Sens. Environ.*, vol. 114, no. 11, pp. 2417–2430, Nov. 2010.

[10] A. Balenzano, F. Mattia, G. Satalino, and M. W. J. Davidson, "Dense temporal series of C- and L-band SAR data for soil moisture retrieval over agricultural crops," *IEEE J. Sel. Topics Appl. Earth Observ. Remote Sens.*, vol. 4, no. 2, pp. 439–450, Jun. 2011.

[11] M. A. Karam and A. K. Fung, "Leaf-shape effects in electromagnetic wave scattering from vegetation," *IEEE Trans. Geosci. Remote Sens.*, vol. 27, no. 6, pp. 687–697, Nov. 1989.

[12] T. Senior, K. Sarabandi, and F. Ulaby, "Measuring and modeling the backscattering cross section of a leaf," *Radio Sci.*, vol. 22, no. 6, pp. 1109–1116, 1987.

[13] K. Sarabandi, T. B. Senior, and F. Ulaby, "Effect of curvature on the backscattering from a leaf," *J. Electromagn. Waves Appl.*, vol. 2, no. 7, pp. 653–670, 1988.

[14] A. McDonald, J. Bennett, G. Cookmartin, S. Crossley, K. Morrison, and S. Quegan, "The effect of leaf geometry on the microwave backscatter from leaves," *Int. J. Remote Sens.*, vol. 21, no. 2, pp. 395–400, 2000.

[15] D. H. Hoekman and B. A. M. Bouman, "Interpretation of C- and X-band radar images over an agricultural area, the Flevoland test site in the Agriscatt-87 campaign," *Int. J. Remote Sens.*, vol. 14, no. 8, pp. 1577–1594, May 1993.

[16] S. H. Yueh, J. A. Kong, J. K. Jao, R. T. Shin, and T. L. Toan, "Branching model for vegetation," *IEEE Trans. Geosci. Remote Sens.*, vol. 30, no. 2, pp. 390–402, Mar. 1992.

[17] M. A. Karam, A. K. Fung, R. H. Lang, and N. S. Chauhan, "A microwave scattering model for layered vegetation," *IEEE Trans. Geosci. Remote Sens.*, vol. 30, no. 4, pp. 767–784, Jul. 1992.

[18] F. T. Ulaby and M. A. El-rayes, "Microwave dielectric spectrum of vegetation—Part II: Dual-dispersion model," *IEEE Trans. Geosci. Remote Sens.*, vol. GE-25, no. 5, pp. 550–557, Sep. 1987.

[19] C. Matzler, "Microwave (1–100 GHz) dielectric model of leaves," *IEEE Trans. Geosci. Remote Sens.*, vol. 32, no. 4, pp. 947–949, Jul. 1994.

[20] G. Picard, T. L. Toan, and F. Mattia, "Understanding C-band radar backscatter from wheat canopy using a multiple-scattering coherent model," *IEEE Trans. Geosci. Remote Sens.*, vol. 41, no. 7, pp. 1583–1591, Jul. 2003.

[21] F. Mattia *et al.*, "Multitemporal C-band radar measurements on wheat fields," *IEEE Trans. Geosci. Remote Sens.*, vol. 41, no. 7, pp. 1551–1560, Jul. 2003.

[22] T. L. Toan *et al.*, "Rice crop mapping and monitoring using ERS-1 data based on experiment and modeling results," *IEEE Trans. Geosci. Remote Sens.*, vol. 35, no. 1, pp. 41–56, Jan. 1997.

[23] X. Blaes, P. Defourny, U. Wegmuller, A. D. Vecchia, L. Guerriero, and P. Ferrazzoli, "C-band polarimetric indexes for maize monitoring based on a validated radiative transfer model," *IEEE Trans. Geosci. Remote Sens.*, vol. 44, no. 4, pp. 791–800, Apr. 2006.

[24] J. Casanova, J. Judge, and M. Jang, "Modeling transmission of microwaves through dynamic vegetation," *IEEE Trans. Geosci. Remote Sens.*, vol. 45, no. 10, pp. 3145–3149, Oct. 2007.

[25] M. S. Moran, P. J. Pinter, B. E. Clothier, and S. G. Allen, "Effect of water stress on the canopy architecture and spectral indices of irrigated alfalfa," *Remote Sens. Environ.*, vol. 29, no. 3, pp. 251–261, 1989. [Online]. Available: http://www.sciencedirect.com/science/article/pii/0034425789900047

[26] D. S. Kimes and J. A. Kirchner, "Diurnal variations of vegetation canopy structure," *Int. J. Remote Sens.*, vol. 4, no. 2, pp. 257–271, Jan. 1983.

[27] T. van Emmerik, S. Steele-Dunne, J. Judge, and N. van de Giesen, "A comparison between leaf dielectric properties of stressed and unstressed tomato plants," in *Proc. 2015 IEEE Int. Geosci. Remote Sens. Symp.*, Jul. 2015, pp. 275–278.

[28] T. van Emmerik, S. C. Steele-Dunne, J. Judge, and N. van de Giesen, "Impact of diurnal variation in vegetation water content on radar backscatter from maize during water stress," *IEEE Trans. Geosci. Remote Sens.*, vol. 53, no. 7, pp. 3855–3869, Jul. 2015.

[29] T. J. Schmugge, "Remote sensing of soil moisture: Recent advances," *IEEE Trans. Geosci. Remote Sens.*, vol. GE-21, no. 3, pp. 336–344, Jul. 1983.

[30] J. R. Wang, E. T. Engman, T. Mo, T. J. Schmugge, and J. Shiue, "The effects of soil moisture, surface roughness, and vegetation on l-band emission and backscatter," *IEEE Trans. Geosci. Remote Sens.*, vol. GE-25, no. 6, pp. 825–833, Nov. 1987.

[31] V. Mironov, M. Dobson, V. Kaupp, S. Komarov, and V. Kleshchenko, "Generalized refractive mixing dielectric model for moist soils," *IEEE Trans. Geosci. Remote Sens.*, vol. 42, no. 4, pp. 773–785, Apr. 2004.

[32] M. C. Dobson, F. T. Ulaby, M. T. Hallikainen, and M. A. El-rayes, "Microwave dielectric behavior of wet soil—Part II: Dielectric mixing models," *IEEE Trans. Geosci. Remote Sens.*, vol. GE-23, no. 1, pp. 35–46, Jan. 1985.

[33] T. F. Bush and F. T. Ulaby, "An evaluation of radar as a crop classifier," *Remote Sens. Environ.*, vol. 7, no. 1, pp. 15–36, Jan. 1978.

[34] H. McNairn and B. Brisco, "The application of C-band polarimetric SAR for agriculture: A review," *Can. J. Remote Sens.*, vol. 30, no. 3, pp. 525–542, 2004.

[35] N. Baghdadi, N. Boyer, P. Todoroff, M. El Hajj, and A. Bgu, "Potential of SAR sensors TerraSAR-X, ASAR/ENVISAT and PALSAR/ALOS for monitoring sugarcane crops on reunion island," *Remote Sens. Environ.*, vol. 113, no. 8, pp. 1724–1738, Aug. 2009.

[36] T. Le Toan *et al.*, "Rice crop mapping and monitoring using ERS-1 data based on experiment and modeling results," *IEEE Trans. Geosci. Remote Sens.*, vol. 35, no. 1, pp. 41–56, Jan. 1997.

[37] H. Skriver *et al.*, "Crop classification using short-revisit Multitemporal SAR data," *IEEE J. Sel. Topics Appl. Earth Observ. Remote Sens.*, vol. 4, no. 2, pp. 423–431, Jun. 2011.

[38] G. Macelloni, S. Paloscia, P. Pampaloni, and E. Santi, "Global scale monitoring of soil and vegetation using SSM/I and ERS wind scatterometer," *Int. J. Remote Sens.*, vol. 24, no. 12, pp. 2409–2425, Jan. 2003.

[39] L. Jarlan *et al.*, "Mapping of Sahelian vegetation parameters from ERS scatterometer data with an evolution strategies algorithm," *Remote Sens. Environ.*, vol. 87, no. 1, pp. 72–84, Sep. 2003.

[40] S. Frolking, T. Milliman, K. McDonald, J. Kimball, M. Zhao, and M. Fahnestock, "Evaluation of the SeaWinds scatterometer for regional monitoring of vegetation phenology," *J. Geophys. Res., Atmospheres*, vol. 111, no. D17, p. D17302, Sep. 2006.

[41] P. Frison and E. Mougin, "Monitoring global vegetation dynamics with ERS-1 wind scatterometer data," *Remote Sens.*, vol. 17, no. 16, pp. 3201–3218, 1996.

[42] M. Abdel-Messeh and S. Quegan, "Variability in ERS scatterometer measurements over land," *IEEE Trans. Geosci. Remote Sens.*, vol. 38, no. 4, pp. 1767–1776, Jul. 2000.

[43] P. J. Hardin and M. W. Jackson, "Investigating SeaWinds terrestrial backscatter," *Photogrammetric Eng. Remote Sens.*, vol. 69, no. 11, pp. 1243–1254, 2003.

[44] L. Guerriero, P. Ferrazzoli, and R. Rahmoune, "A synergyc view of L-band active and passive remote sensing of vegetated soil," in *Proc. 2012 12th Spec. Meeting Microw. Radiometry Remote Sens. Environ.*, Mar. 2012, pp. 1–3.

[45] D. Entekhabi *et al.*, "The soil moisture active passive (SMAP) mission," *Proc. IEEE*, vol. 98, no. 5, pp. 704–716, May 2010.

[46] R. De Jeu, W. Wagner, T. Holmes, A. Dolman, N. Van De Giesen, and J. Friesen, "Global soil moisture patterns observed by space borne microwave radiometers and scatterometers," *Surveys Geophys.*, vol. 29, no. 4-5, pp. 399–420, 2008.

[47] J. Parajka, V. Naeimi, G. Blöschl, and J. Komma, "Matching ERS scatterometer based soil moisture patterns with simulations of a conceptual dual layer hydrologic model over Austria," *Hydrol. Earth Syst. Sci.*, vol. 13, no. 2, pp. 259–271, 2009.

[48] S. Schneider, Y. Wang, W. Wagner, and J.-F. Mahfouf, "Impact of ASCAT soil moisture assimilation on regional precipitation forecasts: A case study for Austria," *Monthly Weather Rev.*, vol. 142, no. 4, pp. 1525–1541, 2014.

[49] N. Wanders, D. Karssenberg, A. D. Roo, S. De Jong, and M. Bierkens, "The suitability of remotely sensed soil moisture for improving operational flood forecasting," *Hydrol. Earth Syst. Sci.*, vol. 18, no. 6, pp. 2343–2357, 2014.

[50] F. Ulaby and R. Moore, "Radar sensing of soil moisture," in *Proc. 1973 Antennas Propag. Soc. Int. Symp.*, vol. 11, Apr. 1973, pp. 362–365.

[51] F. Ulaby, "Radar measurement of soil moisture content," *IEEE Trans. Antennas Propag.*, vol. 22, no. 2, pp. 257–265, Mar. 1974.

[52] E. P. W. Attema and F. T. Ulaby, "Vegetation modeled as a water cloud," *Radio Sci.*, vol. 13, no. 2, pp. 357–364, Mar. 1978.

[53] F. T. Ulaby, A. Aslam, and M. C. Dobson, "Effects of vegetation cover on the radar sensitivity to soil moisture," *IEEE Trans. Geosci. Remote Sens.*, vol. GE-20, no. 4, pp. 476–481, Oct. 1982.

[54] F. Ulaby, "Vegetation clutter model," *IEEE Trans. Antennas Propag.*, vol. 28, no. 4, pp. 538–545, Jul. 1980.

[55] F. T. Ulaby and E. A. Wilson, "Microwave Attenuation Properties of Vegetation Canopies," *IEEE Trans. Geosci. Remote Sens.*, vol. GE-23, no. 5, pp. 746–753, Sep. 1985.

[56] A. Tavakoli, K. Sarabandi, and F. T. Ulaby, "Horizontal propagation through periodic vegetation canopies," *IEEE Trans. Antennas Propag.*, vol. 39, no. 7, pp. 1014–1023, Jul. 1991.

[57] G. P. D. Loor, P. Hoogeboom, and E. P. W. Attema, "The Dutch ROVE program," *IEEE Trans. Geosci. Remote Sens.*, vol. GE-20, no. 1, pp. 3–11, Jan. 1982.

[58] L. Krul, "Some results of microwave remote sensing research in the Netherlands with a view to land applications in the 1990s," *Int. J. Remote Sens.*, vol. 9, no. 10-11, pp. 1553–1563, Oct. 1988.

[59] B. A. M. Bouman and H. W. J. van Kasteren, "Ground-based X-band (3-cm wave) radar backscattering of agricultural crops. I. Sugar beet and potato; backscattering and crop growth," *Remote Sens. Environ.*, vol. 34, no. 2, pp. 93–105, Nov. 1990.

[60] B. A. M. Bouman and H. W. J. van Kasteren, "Ground-based X-band (3-cm wave) radar backscattering of agricultural crops. II. Wheat, barley, and oats; the impact of canopy structure," *Remote Sens. Environ.*, vol. 34, no. 2, pp. 107–119, Nov. 1990.

[61] B. A. M. Bouman, "Crop parameter estimation from ground-based x-band (3-cm wave) radar backscattering data," *Remote Sens. Environ.*, vol. 37, no. 3, pp. 193–205, Sep. 1991.

[62] Y. Inoue *et al.*, "Season-long daily measurements of multifrequency (Ka, Ku, X, C, and L) and full-polarization backscatter signatures over paddy rice field and their relationship with biological variables," *Remote Sens. Environ.*, vol. 81, no. 2, pp. 194–204, 2002.

[63] B. Brisco, R. Brown, J. Gairns, and B. Snider, "Temporal ground-based scatterometer observations of crops in western Canada," *Can. J. Remote Sens.*, vol. 18, no. 1, pp. 14–21, 1992.

[64] B. Brisco, R. Brown, J. Koehler, G. Sofko, and M. Mckibben, "The diurnal pattern of microwave backscattering by wheat," *Remote Sens. Environ.*, vol. 34, no. 1, pp. 37–47, 1990.

[65] A. Toure, K. P. B. Thomson, G. Edwards, R. J. Brown, and B. G. Brisco, "Adaptation of the MIMICS backscattering model to the agricultural context-wheat and canola at L and C bands," *IEEE Trans. Geosci. Remote Sens.*, vol. 32, no. 1, pp. 47–61, Jan. 1994.

[66] D. Major, A. Smith, M. Hill, W. Willms, B. Brisco, and R. Brown, "Radar backscatter and visible infrared reflectance from short-grass prairie," *Can. J. Remote Sens.*, vol. 20, pp. 71–77, 1994.

[67] J. Boisvert, Q. Xu, F. Bonn, R. Brown, and A. Fung, "Modelling backscatter in bare organic soils," in *Proc. 1998 IEEE Int. Geosci. Remote Sens. Symp.*, 1998, vol. 5, pp. 2366–2368.

[68] H. McNairn, J. Boisvert, D. Major, G. Gwyn, R. Brown, and A. Smith, "Identification of agricultural tillage practices from C-band radar backscatter," *Can. J. Remote Sens.*, vol. 22, pp. 154–163, 1996.

[69] H. McNairn, C. Duguay, J. Boisvert, E. Huffman, and B. Brisco, "Defining the sensitivity of multi-frequency and multi-polarized radar backscatter to post-harvest crop residue," *Can. J. Remote Sens.*, vol. 27, pp. 247–263, 2001.

[70] A. Smith and D. Major, "Radar backscatter and crop residues," *Can. J. Remote Sens.*, vol. 22, pp. 243–247, 1996.

[71] B. Brisco, R. J. Brown, B. Snider, G. J. Sofko, J. A. Koehler, and A. G. Wacker, "Tillage effects on the radar backscattering coefficient of grain stubble fields," *Int. J. Remote Sens.*, vol. 12, no. 11, pp. 2283–2298, 1991.

[72] T. Jackson, A. Colliander, J. Kimball, R. Reichle, W. Crow D. Entekhabi, P. O'Neill, and E. Njoku, "SMAP Science Data Calibration and Validation Plan," JPL, (2012). [online]. Available: smap.jpl.nasa.gov/files/smap2/CalVal_Plan_120706_pub.pdf

[73] P. E. O'Neill, R. H. Lang, M. Kurum, C. Utku, and K. R. Carver, "Multi-sensor microwave soil moisture remote sensing: NASA's combined radar/radiometer (ComRAD) system," in *Proc. 2006 IEEE MicroRad*, 2006, pp. 50–54.

[74] M. Kurum, R. H. Lang, P. E. O'Neill, A. T. Joseph, T. J. Jackson, and M. H. Cosh, "L-band radar estimation of forest attenuation for active/passive soil moisture inversion," *IEEE Trans. Geosci. Remote Sens.*, vol. 47, no. 9, pp. 3026–3040, Sep. 2009.

[75] M. Kurum, R. H. Lang, P. E. O'Neill, A. T. Joseph, T. J. Jackson, and M. H. Cosh, "A first-order radiative transfer model for microwave radiometry of forest canopies at L-band," *IEEE Trans. Geosci. Remote Sens.*, vol. 49, no. 9, pp. 3167–3179, Sep. 2011.

[76] P. O'Neill *et al.*, "L-band active / passive time series measurements over a growing season using the ComRAD ground-based SMAP simulator," in *Proc. 2013 IEEE Int. Geosci. Remote Sens. Symp.*, Jul. 2013, pp. 37–40.

[77] P. K. Srivastava, P. O'Neill, M. Cosh, R. Lang, and A. Joseph, "Evaluation of radar vegetation indices for vegetation water content estimation using data from a ground-based SMAP simulator," in *Proc. 2015 IEEE Int. Geosci. Remote Sens. Symp.*, Jul. 2015, pp. 1296–1299.

[78] K. Nagarajan *et al.*, "Automated L-band radar system for sensing soil moisture at high temporal resolution," *IEEE Geosci. Remote Sens. Lett.*, vol. 11, no. 2, pp. 504–508, Feb. 2014.

[79] P.-W. Liu, J. Judge, R. D. DeRoo, A. W. England, T. Bongiovanni, and A. Luke, "Dominant backscattering mechanisms at L-band during dynamic soil moisture conditions for sandy soils," *Remote Sens. Environ.*, vol. 178, pp. 104–112, Jun. 2016.

[80] P. W. Liu, J. Judge, R. DeRoo, A. England, and A. Luke, "Utilizing complementarity of active/passive microwave observations at L-band for soil moisture studies in sandy soils," in *Proc. 2013 IEEE Int. Geosci. Remote Sens. Symp.*, Jul. 2013, pp. 743–746.

[81] P. W. Liu, J. Judge, R. D. D. Roo, A. W. England, and T. Bongiovanni, "Uncertainty in soil moisture retrievals using the SMAP combined active-passive algorithm for growing sweet corn," *IEEE J. Sel. Topics Appl. Earth Observ. Remote Sens.*, vol. 9, no. 7, pp. 3326–3339, Jul. 2016.

[82] A. Monsivais-Huertero, J. Judge, S. Steele-Dunne, and P. W. Liu, "Impact of bias correction methods on estimation of soil moisture when assimilating active and passive microwave observations," *IEEE Trans. Geosci. Remote Sens.*, vol. 54, no. 1, pp. 262–278, Jan. 2016.

[83] J. H. Hwang, S. G. Kwon, and Y. Oh, "Evaluation of calibration accuracy with HPS (Hongik Polarimetric Scatterometer) system for multi-bands and multi-polarizations," in *Proc. 2011 IEEE Int. Geosci. Remote Sens. Symp.*, Jul. 2011, pp. 3987–3990.

[84] Y. Oh and S.-G. Kwon, "Development of a simple scattering model for vegetation canopies and examination of its validity with scatterometer measurements of green-onion fields," in *Proc. 2009 IEEE Int. Geosci. Remote Sens. Symp.*, 2009, pp. II-101–II-104.

[85] S.-G. Kwon, J.-H. Hwang, and Y. Oh, "Soil moisture inversion from X-band SAR and scatterometer data of vegetation fields," in *Proc. 2011 IEEE Int. Geosci. Remote Sens. Symp.*, 2011, pp. 3140–3143.

[86] Y. Oh, S.-Y. Hong, Y. Kim, J.-Y. Hong, and Y.-H. Kim, "Polarimetric backscattering coefficients of flooded rice fields at L- and C-bands: Measurements, modeling, and data analysis," *IEEE Trans. Geosci. Remote Sens.*, vol. 47, no. 8, pp. 2714–2721, Aug. 2009.

[87] S. K. Kweon and Y. Oh, "A modified water-cloud model with leaf angle parameters for microwave backscattering from agricultural fields," *IEEE Trans. Geosci. Remote Sens.*, vol. 53, no. 5, pp. 2802–2809, May 2015.

[88] J. H. Hwang, S. G. Kwon, and Y. Oh, "A rotational high-resolution SAR on a tower at multi-frequencies," in *Proc. 2012 IEEE Int. Geosci. Remote Sens. Symp.*, Jul. 2012, pp. 6891–6894.

[89] P. Snoeij and P. J. Swart, "The DUT airborne scatterometer," *Int. J. Remote Sens.*, vol. 8, no. 11, pp. 1709–1716, 1987.

[90] R. Bernard, D. Vidal-Madjar, F. Baudin, and G. Laurent, "Data processing and calibration for an airborne scatterometer," *IEEE Trans. Geosci. Remote Sens.*, vol. GE-24, no. 5, pp. 709–716, Sep. 1986.

[91] P. Snoeij, P. Swart, and E. Attema, "The general behavior of the radar signature of different european test sites as a function of frequency and polarization," in *Proc. IEEE 10th Annu. Int. Geosci. Remote Sens. Symp.*, 1990, pp. 2315–2318.

[92] B. A. M. Bouman and D. H. Hoekman, "Multi-temporal, multi-frequency radar measurements of agricultural crops during the Agriscatt-88 campaign in The Netherlands," *Int. J. Remote Sens.*, vol. 14, no. 8, pp. 1595–1614, May 1993.

[93] P. Ferrazzoli, S. Paloscia, P. Pampaloni, G. Schiavon, D. Solimini, and P. Coppo, "Sensitivity of microwave measurements to vegetation biomass and soil moisture content: A case study," *IEEE Trans. Geosci. Remote Sens.*, vol. 30, no. 4, pp. 750–756, Jul. 1992.

[94] P. Ferrazzoli, S. Paloscia, P. Pampaloni, G. Schiavon, and D. Solimini, "Multisensor, multifrequency, multitemporal aircraft microwave measurements over agricultural fields," in *Proc. Int. Geosci. Remote Sens. Symp.*, Jun. 1991, vol. 4, pp. 2261–2264.

[95] G. Schoups, P. A. Troch, and N. Verhoest, "Soil moisture influences on the radar backscattering of sugar beet fields," *Remote Sens. Environ.*, vol. 65, no. 2, pp. 184–194, 1998.

[96] L. Prevot, I. Champion, and G. Guyot, "Estimating surface soil moisture and leaf area index of a wheat canopy using a dual-frequency (C and X bands) scatterometer," *Remote Sens. Environ.*, vol. 46, no. 3, pp. 331–339, Dec. 1993.

[97] M. Benallegue *et al.*, "Soil moisture assessment at a basin scale using active microwave remote sensing: the Agriscatt'88 airborne campaign on the Orgeval watershed," *Remote Sens.*, vol. 15, no. 3, pp. 645–656, 1994.

[98] M. Benallegue, O. Taconet, D. Vidal-Madjar, and M. Normand, "The use of radar backscattering signals for measuring soil moisture and surface roughness," *Remote Sens. Environ.*, vol. 53, no. 1, pp. 61–68, 1995.

[99] B. Brisco and R. Brown, "Multidate SAR/TM Synergism for crop classification in Western Canada," *Photogrammetric Eng. Remote Sens.*, vol. 61, pp. 1009–1014, 1995.

[100] B. Brisco and R. Protz, "Corn field identification accuracy using airborne radar imagery," *Can. J. Remote Sens.*, vol. 6, pp. 15–24, 1980.

[101] R. Raney, *Principles and Applications of Imaging Radar, Manual of Remote Sensing*. 3rd ed., New York, NY, USA: Wiley, 1998, vol. 2, pp. 9–130.

[102] H. McNairn, J. Van der Sanden, R. Brown, and J. Ellis, "The potential of RADARSAT-2 for crop mapping and assessing crop condition," in *Proc. 2nd Int. Conf. Geospatial Inf. Agric. Forestry*, Lake Buena Vista, FL, USA, vol. II 2000, pp. 81–88.

[103] H. McNairn, V. Decker, and K. Murnaghan, "The sensitivity of C-Band polarimetric SAR to crop condition," in *Proc.IEEE Int. Geosci. Remote Sens. Symp.*, Jun. 24–28, 2002, pp. 1471–1473.

[104] H. McNairn, K. Hochheim, and N. Rabe, "Applying polarimetric radar imagery for mapping the productivity of wheat crops," *Can. J. Remote Sens.*, vol. 30, no. 3, pp. 517–524, 2004. [Online]. Available: http://www.tandfonline.com/doi/abs/10.5589/m03-068

[105] F. Campbell, R. Ryerson, and R. Brown, "GlobeSAR: A Canadian radar remote sensing program," *Geocarto Int.*, vol. 10, no. 3, pp. 3–7, 1995.

[106] F. Petzinger, "GlobeSAR: The CCRS airborne SAR in the era of RADARSAT," *Geocarto Int.*, vol. 10, no. 3, pp. 9–17, 1995.

[107] R. Brown, M. D'Iorio, and B. Brisco, "GlobeSAR applications review," *Geocarto Int.*, vol. 10, no. 3, pp. 19–31, 1995.

[108] K. Weise and M. W. Davidson, "Dualband-TerraSAR simulation/campaign results for L-band configuration," in *Proc. IEEE Int. Geosci. Remote Sens. Symp.*, 2004, vol. 7, pp. 4556–4559.

[109] G. Satalino, A. Balenzano, F. Mattia, M. Rinaldi, C. Maddaluno, and G. Annicchiarico, "Retrieval of wheat biomass from multitemporal dual polarised SAR observations," in *Proc. 2015 IEEE Int. Geosci. Remote Sens. Symp.*, Jul. 2015, pp. 5194–5197.

[110] A. Burini *et al.*, "Multi-temporal high-resolution polarimetric L-band SAR observation of a wine-producing landscape," in *Proc. 2006 IEEE Int. Symp. Geosci. Remote Sens.*, Jul. 2006, pp. 501–503.

[111] G. Schiavon, D. Solimini, and A. Burini, "Sensitivity of multi-temporal high resolution polarimetric C and L-band SAR to grapes in vineyards," in *Proc. 2007 IEEE Int. Geosci. Remote Sens. Symp.*, Jul. 2007, pp. 3651–3654.

[112] A. Burini, G. Schiavon, and D. Solimini, "Fusion of high resolution polarimetric SAR and multi-spectral optical data for precision viticulure," in *Proc. 2008 IEEE Int. Geosci. Remote Sens. Symp.*, Jul. 2008, vol. 3, pp. III-1000–III-1003.

[113] R. Scheiber *et al.*, "Aquiferex optical and radar campaign-objectives and first results," in *Proc. Eur. Conf. Synthetic Aperture Radar*, VDE Verlag GmbH, Berlin, Offenburg, 2006, p. 4.

[114] Z. Su *et al.*, "EAGLE 2006 Multi-purpose, multi-angle and multi-sensor in-situ and airborne campaigns over grassland and forest," *Hydrol. Earth Syst. Sci.*, vol. 13, no. 6, pp. 833–845, Jun. 2009.

[115] R. Bianchi, M. Davidson, I. Hajnsek, M. Wooding, and C. Wloczyk, "AgriSAR 2006–ESA final report," ESA final report, Noordwijk, Netherlands, 2008.

[116] I. Hajnsek *et al.*, "AgriSAR 2006 Airborne SAR and optics campaigns for an improved monitoring of agricultural processes and practices," *Geophys. Res. Abstr*, vol. 9, p. 04085, 2007.

[117] J. Stamenković, P. Ferrazzoli, L. Guerriero, D. Tuia, and J.-P. Thiran, "Joining a discrete radiative transfer model and a kernel retrieval algorithm for soil moisture estimation from SAR data," *IEEE J. Sel. Topics Appl. Earth Observ. Remote Sens.*, vol. 8, no. 7, pp. 3463–3475, Jul. 2015.

[118] F. Mattia, G. Satalino, V. Pauwels, and A. Loew, "Soil moisture retrieval through a merging of multi-temporal L-band SAR data and hydrologic modelling," *Hydrol. Earth Syst. Sci.*, vol. 13, no. 3, pp. 343–356, 2009.

[119] W. J. Wilson *et al.*, "Passive active L-and S-band (PALS) microwave sensor for ocean salinity and soil moisture measurements," *IEEE Trans. Geosci. Remote Sens.*, vol. 39, no. 5, pp. 1039–1048, May 2001.

[120] A. Colliander *et al.*, "Long term analysis of PALS soil moisture campaign measurements for global soil moisture algorithm development," *Remote Sens. Environ.*, vol. 121, pp. 309–322, 2012.

[121] E. G. Njoku *et al.*, "Observations of soil moisture using a passive and active low-frequency microwave airborne sensor during SGP99," *IEEE Trans. Geosci. Remote Sens.*, vol. 40, no. 12, pp. 2659–2673, Dec. 2002.

[122] U. Narayan, V. Lakshmi, and E. G. Njoku, "Retrieval of soil moisture from passive and active L/S band sensor (PALS) observations during the soil moisture experiment in 2002 (SMEX02)," *Remote Sens. Environ.*, vol. 92, no. 4, pp. 483–496, 2004.

[123] A. Colliander *et al.*, "Comparison of airborne passive and active L-band system (PALS) brightness temperature measurements to SMOS observations during the SMAP validation experiment 2012 (SMAPVEX12)," *IEEE Geosci. Remote Sens. Lett.*, vol. 12, no. 4, pp. 801–805, Apr. 2015.

[124] H. McNairn *et al.*, "The Soil Moisture Active Passive validation experiment 2012 (SMAPVEX12): Prelaunch calibration and validation of the SMAP soil moisture algorithms," *IEEE Trans. Geosci. Remote Sens.*, vol. 53, no. 5, pp. 2784–2801, May 2015.

[125] N. N. Das, D. Entekhabi, E. G. Njoku, J. J. Shi, J. T. Johnson, and A. Colliander, "Tests of the SMAP combined radar and radiometer algorithm using airborne field campaign observations and simulated data," *IEEE Trans. Geosci. Remote Sens.*, vol. 52, no. 4, pp. 2018–2028, Apr. 2014.

[126] M. Piles, D. Entekhabi, and A. Camps, "A change detection algorithm for retrieving high-resolution soil moisture from SMAP radar and radiometer observations," *IEEE Trans. Geosci. Remote Sens.*, vol. 47, no. 12, pp. 4125–4131, Dec. 2009.

[127] D. Gray *et al.*, "PLIS: An airborne polarimetric L-band interferometric synthetic aperture radar," in *Proc. 3rd Int. Asia-Pasific Conf. Synthetic Aperture Radar*, 2011, pp. 1–4.

[128] R. Panciera *et al.*, "The soil moisture active passive experiments (SMAPEX): Toward soil moisture retrieval from the SMAP mission," *IEEE Trans. Geosci. Remote Sens.*, vol. 52, no. 1, pp. 490–507, Jan. 2014.

[129] R. Panciera, M. A. Tanase, K. Lowell, and J. P. Walker, "Evaluation of IEM, Dubois, and Oh radar backscatter models using airborne L-band SAR," *IEEE Trans. Geosci. Remote Sens.*, vol. 52, no. 8, pp. 4966–4979, Aug. 2014.

[130] X. Wu, J. P. Walker, C. Rüdiger, R. Panciera, and D. A. Gray, "Simulation of the SMAP data stream from SMAPEx field campaigns in Australia," *IEEE Trans. Geosci. Remote Sens.*, vol. 53, no. 4, pp. 1921–1934, Apr. 2015.

[131] X. Wu, J. P. Walker, N. N. Das, R. Panciera, and C. Rüdiger, "Evaluation of the SMAP brightness temperature downscaling algorithm using active–passive microwave observations," *Remote Sens. Environ.*, vol. 155, pp. 210–221, 2014.

[132] F. Ulaby, R. More, and A. Fung, *Microwave Remote Sensing: Active and Passive*, Vol. II. Boston, MA, USA: Artech House, 1986.

[133] F. Ulaby and C. Elachi, *Radar Polarimetry for Geoscience Applications*. Norwood, MA, USA: Artech House, 1990.

[134] H. Lievens and N. Verhoest, "On the retrieval of soil moisture in wheat fields from L-band SAR based on water cloud modeling, the IEM, and effective roughness parameters," *IEEE Geosci. Remote Sens. Lett.*, vol. 8, no. 4, pp. 740–744, Jul. 2011.

[135] Y. Inoue, E. Sakaiya, and C. Wang, "Capability of C-band backscattering coefficients from high-resolution satellite SAR sensors to assess biophysical variables in paddy rice," *Remote Sens. Environ.*, vol. 140, pp. 247–266, 2014.

[136] M. Hosseini, H. McNairn, A. Merzouki, and A. Pacheco, "Estimation of leaf area index (LAI) in corn and soybeans using multi-polarization C- and L-band radar data," *Remote Sens. Environ.*, vol. 170, pp. 77–89, 2015.

[137] E. Beriaux, S. Lambot, and P. Defourny, "Estimating surface-soil moisture for retrieving maize leaf-area index from SAR data," *Canadian J. Remote Sens.*, vol. 37, no. 1, pp. 136–150, 2011.

[138] R. Bindlish and A. P. Barros, "Parameterization of vegetation backscatter in radar-based, soil moisture estimation," *Remote Sens. Environ.*, vol. 76, no. 1, pp. 130–137, 2001.

[139] A. Monsivais-Huertero and J. Judge, "Comparison of backscattering models at L-band for growing corn," *IEEE Geosci. Remote Sens. Lett.*, vol. 8, no. 1, pp. 24–28, Jan. 2011.

[140] N. S. Chauhan, R. H. Lang, and K. J. Ranson, "Radar modeling of a boreal forest," *IEEE Trans. Geosci. Remote Sens.*, vol. 29, no. 4, pp. 627–638, Jul. 1991.

[141] S. L. Durden, J. J. Van Zyl, and H. A. Zebker, "Modeling and observation of the radar polarization signature of forested areas," *IEEE Trans. Geosci. Remote Sens.*, vol. 27, no. 3, pp. 290–301, May 1989.

[142] Y. Wang, J. Day, and G. Sun, "Santa Barbara microwave backscatter canopy model for woodlands," *Int. J. Remote Sens.*, vol. 14, no. 8, pp. 1477–1493, 1993.

[143] F. T. Ulaby, K. Sarabandi, K. McDonald, M. Whitt, and M. C. Dobson, "Michigan microwave canopy scattering model," *Int. J. Remote Sens.*, vol. 11, no. 7, pp. 1223–1253, Jul. 1990.

[144] Y. Kerr *et al.*, "Vegetation models and observations: A review," in *Passive Microwave Remote Sensing of Land-Atmosphere Interactions*. Taylor & Francis Ltd., The Netherlands, 1995, pp. 317–344.

[145] S. Chandrasekhar, *Radiative Transfer*. Dover Publications, New York, NY, USA: Courier Corporation, 2013.

[146] P. Ferrazzoli and L. Guerriero, "Radar sensitivity to tree geometry and woody volume: A model analysis," *IEEE Trans. Geosci. Remote Sens.*, vol. 33, no. 2, pp. 360–371, Mar. 1995.

[147] L. Tsang, J. Kong, Z. Chen, K. Pak, and C. Hsu, "Theory of microwave scattering from vegetation based on the collective scattering effects of discrete scatterers," in *Proc. ESA/NASA Int. Workshop Passive Microw. Remote Sens. Res. Related Land-Atmosphere Interactions*, 1995, pp. 117–154.

[148] M. Bracaglia, P. Ferrazzoli, and L. Guerriero, "A fully polarimetric multiple scattering model for crops," *Remote Sens. Environ.*, vol. 54, no. 3, pp. 170–179, 1995.

[149] R. D. D. Roo, Y. Du, F. T. Ulaby, and M. C. Dobson, "A semi-empirical backscattering model at L-band and C-band for a soybean canopy with soil moisture inversion," *IEEE Trans. Geosci. Remote Sens.*, vol. 39, no. 4, pp. 864–872, Apr. 2001.

[150] P.-W. Liu *et al.*, "Assimilation of active and passive microwave observations for improved estimates of soil moisture and crop growth," *IEEE J. Sel. Topics Appl. Earth Observ. Remote Sens.*, vol. 9, no. 4, pp. 1357–1369, Apr. 2016.

[151] P. Ferrazzoli, L. Guerriero, and G. Schiavon, "A vegetation classification scheme validated by model simulations," in *Proc. 1997 IEEE Int. Geosci. Remote Sens. Symp.*, Aug. 1997, vol. 4, pp. 1618–1620.

[152] P. Ferrazzoli, L. Guerriero, and D. Solimini, "Expected performance of a polarimetric bistatic radar for monitoring vegetation," in *Proc. IEEE Int. Geosci. Remote Sens. Symp.*, 2000, vol. 3, pp. 1018–1020.

[153] P. Ferrazzoli, L. Guerriero, A. Quesney, O. Taconet, and J. P. Wigneron, "Investigating the capability of C-band radar to monitor wheat characteristics," in *Proc. IEEE Int. Geosci. Remote Sens. Symp.*, 1999, vol. 2, pp. 723–725.

[154] A. D. Vecchia, P. Ferrazzoli, J. P. Wigneron, and J. P. Grant, "Modeling forest emissivity at L-band and a comparison with multitemporal measurements," *IEEE Geosci. Remote Sens. Lett.*, vol. 4, no. 4, pp. 508–512, Oct. 2007.

[155] A. D. Vecchia *et al.*, "Influence of geometrical factors on crop backscattering at C-band," *IEEE Trans. Geosci. Remote Sens.*, vol. 44, no. 4, pp. 778–790, Apr. 2006.

[156] A. D. Vecchia, P. Ferrazzoli, L. Guerriero, L. Ninivaggi, T. Strozzi, and U. Wegmuller, "Observing and modeling multifrequency scattering of maize during the whole growth cycle," *IEEE Trans. Geosci. Remote Sens.*, vol. 46, no. 11, pp. 3709–3718, Nov. 2008.

[157] L. Thirion, I. Chenerie, and C. Galy, "Application of a coherent model in simulating the backscattering coefficient of a mangrove forest," *Wave Random Media*, vol. 14, no. 2, pp. 393–414, Apr. 2004.

[158] J. M. Stiles and K. Sarabandi, "Electromagnetic scattering from grassland. I. A fully phase-coherent scattering model," *IEEE Trans. Geosci. Remote Sens.*, vol. 38, no. 1, pp. 339–348, Jan. 2000.

[159] J. Stiles and K. Sarabandi, "Electromagnetics scattering from grassland. I. A fully phase-coherent scattering model," *IEEE Trans. Geosci. Remote Sens.*, vol. 38, no. 1, pp. 339–348, Jan. 2000.

[160] J. Stiles, K. Sarabandi, and F. Ulaby, "Electromagnetics scattering from grassland. II. Measurement and modeling results," *IEEE Trans. Geosci. Remote Sens.*, vol. 38, no. 1, pp. 349–356, Jan. 2000.

[161] Y.-C. Lin and K. Sarabandi, "A coherent scattering model for forest canopies based on Monte Carlo simulation of fractal generated trees," in *Proc. IEEE Int. Geosci. Remote Sens. Symp.*, 1996, vol. 2, pp. 1334–1336.

[162] N. S. Chauhan, D. M. L. Vine, and R. H. Lang, "Discrete scatter model for microwave radar and radiometer response to corn: Comparison of theory and data," *IEEE Trans. Geosci. Remote Sens.*, vol. 32, no. 2, pp. 416–426, Mar. 1994.

[163] C. Liu, J. Shang, P. Vachon, and H. McNairn, "Multiyear crop monitoring using polarimetric RADARSAT-2 data," *IEEE Trans. Geosci. Remote Sens.*, vol. 51, no. 4, pp. 2227–2240, Apr. 2013.

[164] A. Freeman and S. L. Durden, "A three-component scattering model for polarimetric SAR data," *IEEE Trans. Geosci. Remote Sens.*, vol. 36, no. 3, pp. 963–973, May 1998.

[165] Y. Yamaguchi, A. Sato, W. Boerner, R. Sato, and H. Yamada, "Four-component scattering power decomposition with rotation of coherence matrix," *IEEE Trans. Geosci. Remote Sens.*, vol. 49, no. 6, pp. 2251–2258, Jun. 2011.

[166] A. Sato, Y. Yamaguchi, G. Singh, and S.-E. Park, "Four-component scattering power decomposition with extended volume scattering model," *IEEE Geosci. Remote Sens. Lett.*, vol. 9, no. 2, pp. 166–170, Mar. 2012.

[167] J. Lee and L. Thomas, "The effect of orientation angle compensation on coherency matrix and polarimetric target decompositions," *IEEE Trans. Geosci. Remote Sens.*, vol. 49, no. 1, pp. 53–64, Jan. 2011.

[168] S. Cloude and E. Pottier, "An entropy based classification scheme for land applications of polarimetric SAR," *IEEE Trans. Geosci. Remote Sens.*, vol. 35, no. 1, pp. 68–78, Jan. 1997.

[169] V. Alberga, G. Satalino, and D. Staykova, "Comparison of polarimetric SAR observables in terms of classification performance," *Int. J. Remote Sens.*, vol. 29, no. 14, pp. 4129–4150, 2008.

[170] J. Lee and E. Pottier, *Polarimetric Radar Imaging: From Basics to Applications*. New York, NY, USA: CRC Press, 2009.

[171] J. M. Lopez-Sanchez, F. Vicente-Guijalba, J. D. Ballester-Berman, and S. R. Cloude, "Polarimetric response of rice fields at C-Band: Analysis and phenology retrieval," *IEEE Trans. Geosci. Remote Sens.*, vol. 52, no. 5, pp. 2977–2993, May 2014.

[172] J. R. Adams, T. L. Rowlandson, S. J. McKeown, A. A. Berg, H. McNairn, and S. J. Sweeney, "Evaluating the Cloude–Pottier and Freeman–Durden scattering decompositions for distinguishing between unharvested and post-harvest agricultural fields," *Can. J. Remote Sens.*, vol. 39, no. 4, pp. 318–327, Oct. 2013.

[173] I. H. Woodhouse and D. H. Hoekman, "Determining land-surface parameters from the ERS wind scatterometer," *IEEE Trans. Geosci. Remote Sens.*, vol. 38, no. 1, pp. 126–140, Jan. 2000.

[174] I. H. Woodhouse and D. H. Hoekman, "A model-based determination of soil moisture trends in Spain with the ERS-scatterometer," *IEEE Trans. Geosci. Remote Sens.*, vol. 38, no. 4, pp. 1783–1793, Jul. 2000.

[175] P. L. Frison, E. Mougin, L. Jarlan, M. A. Karam, and P. Hiernaux, "Comparison of ERS wind-scatterometer and SSM/I data for Sahelian vegetation monitoring," *IEEE Trans. Geosci. Remote Sens.*, vol. 38, no. 4, pp. 1794–1803, Jul. 2000.

[176] L. Jarlan, P. Mazzega, and E. Mougin, "Retrieval of land surface parameters in the Sahel from ERS wind scatterometer data: A "brute force" method," *IEEE Trans. Geosci. Remote Sens.*, vol. 40, no. 9, pp. 2056–2062, Sep. 2002.

[177] L. Jarlan *et al.*, "Mapping of Sahelian vegetation parameters from ERS scatterometer data with an evolution strategies algorithm," *Remote Sens. Environ.*, vol. 87, no. 1, pp. 72–84, 2003.

[178] M. Grippa and I. H. Woodhouse, "Retrieval of bare soil and vegetation parameters from wind scatterometer measurements over three different climatic regions," *Remote Sens. Environ.*, vol. 84, no. 1, pp. 16–24, 2003.

[179] L. Lu, H. Guo, C. Wang, and Q. Li, "Assessment of the SeaWinds scatterometer for vegetation phenology monitoring across china," *Int. J. Remote Sens.*, vol. 34, no. 15, pp. 5551–5568, 2013.

[180] N. Ringelmann, K. Scipal, Z. Bartalis, and W. Wagner, "Planting date estimation in semi-arid environments based on Ku-band radar scatterometer data," in *Proc. IEEE Int. Geosci. Remote Sens. Symp.*, Sep. 2004, vol. 2, pp. 1288–1291.

[181] P. J. Hardin and M. W. Jackson, "Examining vegetation phenological change in South America using reconstructed SeaWinds data: Grasslands and savanna," in *Proc. IEEE Int. Geosci. Remote Sens. Symp.*, 2002, vol. 6, pp. 3296–3298.

[182] T. L. Toan *et al.*, "Rice crop mapping and monitoring using ERS-1 data based on experiment and modeling results," *IEEE Trans. Geosci. Remote Sens.*, vol. 35, no. 1, pp. 41–56, Jan 1997.

[183] F. Ribbes, "Rice field mapping and monitoring with RADARSAT data," *Int. J. Remote Sens.*, vol. 20, no. 4, pp. 745–765, 1999.

[184] A. Bouvet, T. L. Toan, and N. L. Dao, "Estimation of agricultural and biophysical parameters of rice fields in Vietnam using X-band dual-polarization SAR," in *Proc. 2014 IEEE Geosci. Remote Sens. Symp.*, Jul. 2014, pp. 1504–1507.

[185] H. McNairn, A. Kross, D. Lapen, R. Caves, and J. Shang, "Early season monitoring of corn and soybeans with TerraSAR-X and RADARSAT-2," *Int. J. Appl. Earth Observ. Geoinf.*, vol. 28, pp. 252–259, 2014.

[186] H. McNairn, J. Shang, X. Jiao, and C. Champagne, "The contribution of ALOS PALSAR multipolarization and polarimetric data to crop classification," *IEEE Trans. Geosci. Remote Sens.*, vol. 47, no. 12, pp. 3981–3992, Dec. 2009.

[187] B. Deschamps, H. McNairn, J. Shang, and X. Jiao, "Towards operational radar-only crop type classification: Comparison of a traditional decision tree with a random forest classifier," *Can. J. Remote Sens.*, vol. 38, no. 1, pp. 60–68, 2012.

[188] C. Chen and H. McNairn, "A neural network integrated approach for rice crop monitoring," *Int. J. Remote Sens.*, vol. 27, no. 7, pp. 1367–1393, 2006.

[189] Y. Zhang, C. Wang, J. Wu, J. Qi, and W. A. Salas, "Mapping paddy rice with multitemporal ALOS/PALSAR imagery in southeast China," *Int. J. Remote Sens.*, vol. 30, no. 23, pp. 6301–6315, 2009.

[190] S. C. Liew, S.-P. Kam, T.-P. Tuong, P. Chen, V. Q. Minh, and H. Lim, "Application of multitemporal ERS-2 synthetic aperture radar in delineating rice cropping systems in the Mekong River Delta, Vietnam," *IEEE Trans. Geosci. Remote Sens.*, vol. 36, no. 5, pp. 1412–1420, Sep. 1998.

[191] K. Jia, Q. Li, Y. Tian, B. Wu, F. Zhang, and J. Meng, "Crop classification using multi-configuration SAR data in the North China Plain," *Int. J. Remote Sens.*, vol. 33, pp. 170–183, 2012.

[192] H. Skriver, "Crop classification by multitemporal C- and L-band single- and dual-polarization and fully polarimetric SAR," *IEEE Trans. Geosci. Remote Sens.*, vol. 50, no. 6, pp. 2138–2149, Jun. 2012.

[193] M. C. Dobson, L. E. Pierce, and F. T. Ulaby, "Knowledge-based land-cover classification using ERS-1/JERS-1 SAR composites," *IEEE Trans. Geosci. Remote Sens.*, vol. 34, no. 1, pp. 83–99, Jan. 1996.

[194] K. Chen, W. Huang, D. Tsay, and F. Amar, "Classification of multi-frequency polarimetric SAR imagery using a dynamic learning neural network," *IEEE Trans. Geosci. Remote Sens.*, vol. 34, no. 3, pp. 814–820, May 1996.

[195] P. Ferrazzoli, S. Paloscia, P. Pampaloni, G. Schiavon, S. Sigismondi, and D. Solimini, "The potential of multifrequency polarimetric SAR in assessing agricultural and arboreous biomass," *IEEE Trans. Geosci. Remote Sens.*, vol. 35, no. 1, pp. 5–17, Jan. 1997.

[196] P. Ferrazzoli, L. Guerriero, and G. Schiavon, "Experimental and model investigation on radar classification capability," *IEEE Trans. Geosci. Remote Sens.*, vol. 37, no. 2, pp. 960–968, Mar. 1999.

[197] M. Hill, C. Ticehurst, J.-S. Lee, M. Grunes, G. Donald, and D. Henry, "Integration of optical and radar classifications for mapping pasture type in Western Australia," *IEEE Trans. Geosci. Remote Sens.*, vol. 43, no. 7, pp. 1665–1681, Jul. 2005.

[198] D. H. Hoekman, M. A. M. Vissers, and T. N. Tran, "Unsupervised full-p SAR data segmentation as a tool for classification of agricultural areas," *IEEE J. Sel. Topics Appl. Earth Observ. Remote Sens.*, vol. 4, no. 2, pp. 402–411, Jun. 2011.

[199] G. Foody, M. McCulloch, and W. Yates, "Crop classification from C-band polarimetric radar data," *Int. J. Remote Sens.*, vol. 15, no. 14, pp. 2871–2885, 1994.

[200] J.-S. Lee, M. Grunes, and E. Pottier, "Quantitative comparison of classification capability: Fully polarimetric versus dual and single-polarization SAR," *IEEE Trans. Geosci. Remote Sens.*, vol. 39, no. 11, pp. 2343–2351, Nov. 2001.

[201] H. McNairn, C. Champagne, J. Shang, D. Holmstrom, and G. Reichert, "Integration of optical and synthetic aperture radar (SAR) imagery for delivering operational annual crop inventories," *ISPRS J. Photogrammetry Remote Sens.*, vol. 64, pp. 434–449, 2009.

[202] T. Fisette *et al.*, "AAFC annual crop inventory: Status and challenges," in *Proc. 2nd Int. Conf. Agro-Geoinformat.*, Aug. 12–16, 2013, pp. 270–274.

[203] D. Hoekman and A. Vissers, "A new polarimetric classification approach evaluated for agricultural crops," *IEEE Trans. Geosci. Remote Sens.*, vol. 41, no. 12, pp. 2881–2889, Dec. 2003.

[204] F. Charbonneau *et al.*, "Compact polarimetry overview and applications assessment," *Can. J. Remote Sens.*, vol. 36, no. 2, pp. 298–315, 2010.

[205] A. Chipanshi *et al.*, "Evaluation of the integrated Canadian crop yield forecaster (ICCYF) model for in-season prediction of crop yield across the Canadian agricultural landscape," *Agricultural Forest Meteorol.*, vol. 206, pp. 137–150, 2015.

[206] J. Liu, E. Pattey, J. Miller, H. McNairn, and A. Smith, "Estimating crop stresses, aboveground dry biomass and yield of corn using multi-temporal optical data combined with a radiation use efficiency model," *Remote Sens. Environ.*, vol. 114, no. 6, pp. 1167–1177, 2010.

[207] F. Ulaby, C. Allen, G. Eger III, and E. Kanemasu, "Relating the microwave backscattering coefficient to leaf area index," *Remote Sens. Environ.*, vol. 14, pp. 113–133, 1984.

[208] J. F. Paris, "Probing thick vegetation canopies with a field microwave scatterometer," *IEEE Trans. Geosci. Remote Sens.*, vol. GE-24, no. 6, pp. 886–893, Nov. 1986.

[209] H. McNairn, J. Shang, X. Jiao, and B. Deschamps, "Establishing crop productivity using RADARSAT-2," *Int. Arch. Photogramm. Remote Sens. Spat. Inf. Sci.,* vol. 39-B8, pp. 283–287, 2012.

[210] X. Jiao, H. McNairn, J. Shang, E. Pattey, J. Liu, and C. Champagne, "The sensitivity of RADARSAT-2 polarimetric SAR data to corn and soybean leaf area index," *Can. J. Remote Sens.*, vol. 37, no. 1, pp. 69–81, 2011.

[211] S. Maity, C. Patnaik, M. Chakraborty, and S. Panigrahy, "Analysis of temporal backscattering of cotton crops using a semiempirical model," *IEEE Trans. Geosci. Remote Sens.*, vol. 42, no. 3, pp. 577–587, Mar. 2004.

[212] R. Prasad, "Estimation of kidney bean crop variables using ground-based scatterometer data at 9.89 GHz," *Int. J. Remote Sens.*, vol. 32, pp. 31–48, 2011.

[213] Y. Kim, T. Jackson, R. Bindlish, H. Lee, and S. Hong, "Monitoring soybean growth using L-, C-, and X-band scatterometer data," *Int. J. Remote Sens.*, vol. 34, no. 11, pp. 4069–4082, Jun. 2013.

[214] G. Wiseman, H. McNairn, S. Homayouni, and J. Shang, "RADARSAT-2 polarimetric SAR response to crop biomass for agricultural production monitoring," *IEEE J. Sel. Topics Appl. Earth Observ. Remote Sens.*, vol. 7, no. 11, pp. 4461–4471, Nov. 2014.

[215] S. Paloscia, "A summary of experimental results to assess the contribution of SAR for mapping vegetation biomass and soil moisture," *Can. J. Remote Sens.*, vol. 28, no. 2, pp. 246–261, 2002.

[216] M. Moran, J. Moreno, M. Mateo, D. de la Cruz, and A. Montoro, "A RADARSAT-2 quad- polarized time series for monitoring crop and soil conditions in Barrax, Spain," *IEEE Trans. Geosci. Remote Sens.*, vol. 50, no. 4, pp. 1057–1070, Apr. 2012.

[217] G. Satalino, L. Dente, and F. Mattia, "Integration of MERIS and ASAR data for LAI estimation of wheat fields," *2006 IEEE Int. Symp. Geosci. Remote Sens.*, pp. 2255–2258, 2006.

[218] J. Chen, H. Lin, C. Huang, and C. Fang, "The relationship between the leaf area index (LAI) of rice and the C-band SAR vertical/horizontal (VV/HH) polarization ratio," *Int. J. Remote Sens.*, vol. 30, no. 8, pp. 2149–2154, Apr. 2009.

[219] H. Lin, J. Chen, Z. Pei, S. Zhang, and X. Hu, "Monitoring sugarcane growth using ENVISAT ASAR data," *IEEE Trans. Geosci. Remote Sens.*, vol. 47, no. 8, pp. 2572–2580, Aug. 2009.

[220] Y. Kim and J. J. van Zyl, "A time-series approach to estimate soil moisture using polarimetric radar data," *IEEE Trans. Geosci. Remote Sens.*, vol. 47, no. 8, pp. 2519–2527, Aug. 2009.

[221] J. Shang *et al.*, "Tracking crop phenological development of spring wheat using synthetic aperture radar (SAR) in northern Ontario, Canada," in *Proc. 2nd Int. Conf. Agro-Geoinformat.*, Aug. 2013, pp. 517–521.

[222] J. Shang *et al.*, "Using earth observation to monitor corn growth in eastern canada," *68th North Eastern Corn Improvement Conf.*, Wooster, Ohio, USA, Feb. 13–14, 2014.

[223] Y. Kim, T. Jackson, R. Bindlish, H. Lee, and S. Hong, "Radar vegetation index for estimating the vegetation water content of rice and soybean," *IEEE Geosci. Remote Sens. Lett.*, vol. 9, no. 4, pp. 564–568, Jul. 2012.

[224] P. Narvekar, D. Entekhabi, S.-B. Kim, and E. Njoku, "Soil moisture retrieval using L-band radar observations," *IEEE Trans. Geosci. Remote Sens.*, vol. 53, no. 6, pp. 3492–3506, Jun. 2015.

[225] A. Kross, H. McNairn, D. Lapen, M. Sunohara, and C. Champagne, "Assessment of RapidEye vegetation indices for estimation of leaf area index and biomass in corn and soybean crops," *Int. J. Appl. Earth Observ. Geoinf.*, vol. 34, pp. 235–248, 2015.

[226] J. M. Lopez-Sanchez, J. D. Ballester-Berman, and I. Hajnsek, "First results of rice monitoring practices in spain by means of time series of TerraSAR-X dual-pol images," *IEEE J. Sel. Topics Appl. Earth Observ. Remote Sens.*, vol. 4, no. 2, pp. 412–422, Jun. 2011.

[227] J. M. Lopez-Sanchez, S. R. Cloude, and J. D. Ballester-Berman, "Rice phenology monitoring by means of SAR polarimetry at X-Band," *IEEE Trans. Geosci. Remote Sens.*, vol. 50, no. 7, pp. 2695–2709, Jul. 2012.

[228] J. M. Lopez-Sanchez, F. Vicente-Guijalba, J. D. Ballester-Berman, and S. R. Cloude, "Polarimetric response of rice fields at C-band: Analysis and phenology retrieval," *IEEE Trans. Geosci. Remote Sens.*, vol. 52, no. 5, pp. 2977–2993, May 2014.

[229] Z. Yang, K. Li, L. Liu, Y. Shao, B. Brisco, and W. Li, "Rice growth monitoring using simulated compact polarimetric C band SAR," *Radio Sci.*, vol. 49, no. 12, pp. 1300–1315, 2014.

[230] Y. Shao *et al.*, "Rice monitoring and production estimation using multitemporal RADARSAT," *Remote Sens. Environ.*, vol. 76, no. 3, pp. 310–325, 2001.

[231] O. Yuzugullu, E. Erten, and I. Hajnsek, "Rice growth monitoring by means of X-band co-polar SAR: Feature clustering and BBCH scale," *IEEE Geosci. Remote Sens. Lett.*, vol. 12, no. 6, pp. 1218–1222, Jun. 2015.

[232] L. Mascolo, J. Lopez-Sanchez, F. Vicente-Guijalba, G. Mazzarella, F. Nunziata, and M. Migliaccio, "Retrieval of phenological stages of onion fields during the first year of growth by means of C-band polarimetric SAR measurements," *Int. J. Remote Sens.*, vol. 36, no. 12, pp. 3077–3096, 2015.

[233] F. Nunziata, M. Migliaccio, J. M. L. Sanchez, L. Mascolo, G. Mazzarella, and G. D'Urso, "C-band polarimetric SAR measurements for the monitoring of growth stages of corn fields in the piana DEL sele zone," in *Proc. 2015 IEEE Int. Geosci. Remote Sens. Symp.*, Jul. 2015, pp. 3377–3380.

[234] L. Zhao, J. Yang, P. Li, and L. Zhang, "Characteristics analysis and classification of crop harvest patterns by exploiting high-frequency multipolarization SAR data," *IEEE J. Sel. Topics Appl. Earth Observ. Remote Sens.*, vol. 7, no. 9, pp. 3773–3783, Sep. 2014.

[235] F. Vicente-Guijalba, T. Martinez-Marin, and J. M. Lopez-Sanchez, "Dynamical approach for real-time monitoring of agricultural crops," *IEEE Trans. Geosci. Remote Sens.*, vol. 53, no. 6, pp. 3278–3293, Jun. 2015.

[236] C. D. Bernardis, F. Vicente-Guijalba, T. Martinez-Marin, and J. M. Lopez-Sanchez, "Contribution to real-time estimation of crop phenological states in a dynamical framework based on NVDI time series: Data fusion with SAR and temperature," *IEEE J. Sel. Topics Appl. Earth Observ. Remote Sens.*, vol. 9, no. 8, pp. 3512–3523, Aug. 2016.

[237] C. G. De Bernardis, F. Vicente-Guijalba, T. Martinez-Marin, and J. M. Lopez-Sanchez, "Estimation of key dates and stages in rice crops using dual-polarization SAR time series and a particle filtering approach," *IEEE J. Sel. Topics Appl. Earth Observ. Remote Sens.*, vol. 8, no. 3, pp. 1008–1018, Mar. 2015.

[238] F. Vicente-Guijalba, T. Martinez-Marin, and J. M. Lopez-Sanchez, "Crop phenology estimation using a multitemporal model and a Kalman filtering strategy," *IEEE Geosci. Remote Sens. Lett.*, vol. 11, no. 6, pp. 1081–1085, Jun. 2014.

[239] L. Mascolo, J. M. Lopez-Sanchez, F. Vicente-Guijalba, F. Nunziata, M. Migliaccio, and G. Mazzarella, "A complete procedure for crop phenology estimation with PolSAR data based on the complex Wishart classifier," *IEEE Trans. Geosci. Remote Sens.*, vol. 54, no. 11, pp. 6505–6515, Nov. 2016.

[240] J. M. Lopez-Sanchez and J. D. Ballester-Berman, "Potentials of polarimetric SAR interferometry for agriculture monitoring," *Radio Sci.*, vol. 44, no. 2, p. 1–20, Apr. 2009.

[241] A. Ceballos, K. Scipal, W. Wagner, and J. Martnez-Fernndez, "Validation of ERS scatterometer-derived soil moisture data in the central part of the Duero Basin, Spain," *Hydrological Processes*, vol. 19, no. 8, pp. 1549–1566, May 2005. [Online]. Available: http://onlinelibrary.wiley.com/doi/10.1002/hyp.5585/abstract

[242] J. D. Bolten, W. T. Crow, X. Zhan, T. J. Jackson, and C. A. Reynolds, "Evaluating the utility of remotely sensed soil moisture retrievals for operational agricultural drought monitoring," *IEEE J. Sel. Topics Appl. Earth Observ. Remote Sens.*, vol. 3, no. 1, pp. 57–66, Mar. 2010.

[243] W. Wagner *et al.*, "Assessing water-limited crop production with a scatterometer based crop growth monitoring system," in *Proc. IEEE Int. Geosci. Remote Sens. Symp.*, 2000, vol. 4, pp. 1696–1698.

[244] A. D. De Wit and C. Van Diepen, "Crop model data assimilation with the ensemble Kalman filter for improving regional crop yield forecasts," *Agricultural Forest Meteorol.*, vol. 146, no. 1, pp. 38–56, 2007.

[245] S. Chakrabarti, T. Bongiovanni, J. Judge, L. Zotarelli, and C. Bayer, "Assimilation of SMOS soil moisture for quantifying drought impacts on crop yield in agricultural regions," *IEEE J. Sel. Topics Appl. Earth Observ. Remote Sens.*, vol. 7, no. 9, pp. 3867–3879, Sep. 2014.

[246] W. Wagner *et al.*, "The ASCAT soil moisture product: A review of its specifications, validation results, and emerging applications," *Meteorologische Zeitschrift*, vol. 22, no. 1, pp. 5–33, Feb. 2013.

[247] W. Wagner, G. Lemoine, M. Borgeaud, and H. Rott, "A study of vegetation cover effects on ERS scatterometer data," *IEEE Trans. Geosci. Remote Sens.*, vol. 37, no. 2, pp. 938–948, Mar. 1999.

[248] W. Wagner, G. Lemoine, and H. Rott, "A method for estimating soil moisture from ERS scatterometer and soil data," *Remote Sens. Environ.*, vol. 70, no. 2, pp. 191–207, 1999.

[249] W. Wagner and K. Scipal, "Large-scale soil moisture mapping in western Africa using the ERS scatterometer," *IEEE Trans. Geosci. Remote Sens.*, vol. 38, no. 4, pp. 1777–1782, Jul. 2000.

[250] W. Wagner, K. Scipal, C. Pathe, D. Gerten, W. Lucht, and B. Rudolf, "Evaluation of the agreement between the first global remotely sensed soil moisture data with model and precipitation data," *J. Geophys. Res., Atmospheres*, vol. 108, no. D19, p. 4611, Oct. 2003.

[251] Z. Bartalis *et al.*, "Initial soil moisture retrievals from the METOP-A advanced scatterometer (ASCAT)," *Geophys. Res. Lett.*, vol. 34, no. 20, p. L20401, Oct. 2007.

[252] V. Naeimi, K. Scipal, Z. Bartalis, S. Hasenauer, and W. Wagner, "An improved soil moisture retrieval algorithm for ERS and METOP scatterometer observations," *IEEE Trans. Geosci. Remote Sens.*, vol. 47, no. 7, pp. 1999–2013, Jul. 2009.

[253] W. Dorigo *et al.*, "Evaluation of the ESA CCI soil moisture product using ground-based observations," *Remote Sens. Environ.*, vol. 162, pp. 380–395, Jun. 2015.

[254] M. Vreugdenhil, W. A. Dorigo, W. Wagner, R. A. M. D. Jeu, S. Hahn, and M. J. E. V. Marle, "Analyzing the vegetation parameterization in the TU-Wien ASCAT soil moisture retrieval," *IEEE Trans. Geosci. Remote Sens.*, vol. 54, no. 6, pp. 3513–3531, Jun. 2016.

[255] S.-B. Kim, L. Tsang, J. T. Johnson, S. Huang, J. J. van Zyl, and E. G. Njoku, "Soil moisture retrieval using time-series radar observations over bare surfaces," *IEEE Trans. Geosci. Remote Sens.*, vol. 50, no. 5, pp. 1853–1863, May 2012.

[256] S.-B. Kim, M. Moghaddam, L. Tsang, M. Burgin, X. Xu, and E. G. Njoku, "Models of L-band radar backscattering coefficients over global terrain for soil moisture retrieval," *IEEE Trans. Geosci. Remote Sens.*, vol. 52, no. 2, pp. 1381–1396, Feb. 2014.

[257] Y. Kim and J. van Zyl, "A time-series approach to estimate soil moisture using polarimetric radar data," *IEEE Trans. Geosci. Remote Sens.*, vol. 47, no. 8, pp. 2519–2527, Aug. 2009.

[258] D. G. Long and P. J. Hardin, "Vegetation studies of the Amazon basin using enhanced resolution Seasat scatterometer data," *IEEE Trans. Geosci. Remote Sens.*, vol. 32, no. 2, pp. 449–460, Mar. 1994.

[259] D. G. Long, P. J. Hardin, and P. T. Whiting, "Resolution enhancement of spaceborne scatterometer data," *IEEE Trans. Geosci. Remote Sens.*, vol. 31, no. 3, pp. 700–715, May 1993.

[260] J.-F. Mahfouf, "Assimilation of satellite-derived soil moisture from ASCAT in a limited-area NWP model," *Quart. J. Roy. Meteorological Soc.*, vol. 136, no. 648, pp. 784–798, Apr. 2010.

[261] K. Scipal, M. Drusch, and W. Wagner, "Assimilation of a ERS scatterometer derived soil moisture index in the ECMWF numerical weather prediction system," *Adv. Water Resources*, vol. 31, no. 8, pp. 1101–1112, 2008.

[262] V. R. Pauwels, R. Hoeben, N. E. Verhoest, F. P. De Troch, and P. A. Troch, "Improvement of TOPLATS-based discharge predictions through assimilation of ERS-based remotely sensed soil moisture values," *Hydrological Processes*, vol. 16, no. 5, pp. 995–1013, 2002.

[263] W. Wagner *et al.*, "Temporal stability of soil moisture and radar backscatter observed by the advanced synthetic aperture radar (ASAR)," *Sensors*, vol. 8, no. 2, pp. 1174–1197, Feb. 2008.

[264] J. C. Friesen, "Regional vegetation water effects on satellite soil moisture estimations for West Africa," Ph.D. thesis, Delft University of Technology, Delft, Netherlands, 2008.

[265] S. C. Steele-Dunne, J. Friesen, and N. van de Giesen, "Using diurnal variation in backscatter to detect vegetation water stress," *IEEE Trans. Geosci. Remote Sens.*, vol. 50, no. 7, pp. 2618–2629, Jul. 2012.

[266] I. Birrer, E. Bracalente, G. Dome, J. Sweet, and G. Berthold, "σ^0 signature of the Amazon rain forest obtained from the Seasat scatterometer," *IEEE Trans. Geosci. Remote Sens.*, vol. GE-20, no. 1, pp. 11–17, Jan. 1982.

[267] M. Satake and H. Hanado, "Diurnal change of Amazon rain forest σ^0 observed by Ku-band spaceborne radar," *IEEE Trans. Geosci. Remote Sens.*, vol. 42, no. 6, pp. 1127–1134, Jun. 2004.

[268] S. Jaruwatanadilok and B. W. Stiles, "Trends and variation in Ku-band backscatter of natural targets on land observed in QuikSCAT data," *IEEE Trans. Geosci. Remote Sens.*, vol. 52, no. 7, pp. 4383–4390, Jul. 2014.

[269] F. Ulaby and P. Batlivala, "Diurnal variations of radar backscatter from a vegetation canopy," *IEEE Trans. Antennas Propag.*, vol. 24, no. 1, pp. 11–17, Jan. 1976.

[270] R. Schroeder, K. C. McDonald, M. Azarderakhsh, and R. Zimmermann, "ASCAT MetOp-A diurnal backscatter observations of recent vegetation drought patterns over the contiguous U.S.: An assessment of spatial extent and relationship with precipitation and crop yield," *Remote Sens. Environ.*, vol. 177, pp. 153–159, May 2016.

[271] W. Wagner *et al.*, "The ASCAT soil moisture product: A review of its specifications, validation results, and emerging applications," *Meteorologische Zeitschrift*, vol. 22, no. 1, pp. 5–33, 2013.

[272] J. Way *et al.*, "Diurnal change in trees as observed by optical and microwave sensors: The EOS synergism study," *IEEE Trans. Geosci. Remote Sens.*, vol. 29, no. 6, pp. 807–821, Nov. 1991.
[273] J. Friesen, H. C. Winsemius, R. Beck, K. Scipal, W. Wagner, and N. Van De Giesen, "Spatial and seasonal patterns of diurnal differences in ERS Scatterometer soil moisture data in the Volta Basin, West Africa," *IAHS Publication*, vol. 316, p. 47, 2007.
[274] K. C. McDonald, R. Zimmermann, and J. S. Kimball, "Diurnal and spatial variation of xylem dielectric constant in Norway Spruce (Picea abies [L.] Karst.) as related to microclimate, xylem sap flow, and xylem chemistry," *IEEE Trans. Geosci. Remote Sens.*, vol. 40, no. 9, pp. 2063–2082, Sep. 2002.
[275] R. Torres *et al.*, "GMES Sentinel-1 mission," *Remote Sens. Environ.*, vol. 120, pp. 9–24, May 2012.
[276] A. A. Thompson, "Overview of the RADARSAT constellation mission," *Can. J. Remote Sens.*, vol. 41, no. 5, pp. 401–407, 2015.
[277] "NASA focused on sentinel as replacement for SMAP radar," Nov. 2015. [Online]. Available: http://spacenews.com/nasa-focused-on-sentinel-as-replacement-for-smap-radar/
[278] S. C. M. Brown, S. Quegan, K. Morrison, J. C. Bennett, and G. Cookmartin, "High-resolution measurements of scattering in wheat canopies-implications for crop parameter retrieval," *IEEE Trans. Geosci. Remote Sens.*, vol. 41, no. 7, pp. 1602–1610, Jul. 2003.
[279] H. Jörg, M. Pardini, I. Hajnsek, and K. P. Papathanassiou, "First multifrequency investigation of SAR tomography for vertical structure of agricultural crops," in *Proc. 10th Eur. Conf. Synthetic Aperture Radar*, 2014, pp. 1–4.
[280] H. Joerg, M. Pardini, K. P. Papathanassiou, and I. Hajnsek, "Analysis of orientation effects of crop vegetation volumes by means of SAR tomography at different frequencies," in *Proc. 11th Eur. Conf. Synthetic Aperture Radar.*, 2016, pp. 1–4.
[281] A. Reigber and A. Moreira, "First demonstration of airborne SAR tomography using multibaseline L-band data," *IEEE Trans. Geosci. Remote Sens.*, vol. 38, no. 5, pp. 2142–2152, Sep. 2000.
[282] M. Pardini, A. T. Caicoya, F. Kugler, S.-K. Lee, I. Hajnsek, and K. Papathanassiou, "On the estimation of forest vertical structure from multibaseline polarimetric SAR data," in *Proc. 2012 IEEE Int. Geosci. Remote Sens. Symp.*, 2012, pp. 3443–3446.
[283] E. Aguilera, M. Nannini, and A. Reigber, "Wavelet-based compressed sensing for SAR tomography of forested areas," *IEEE Trans. Geosci. Remote Sens.*, vol. 51, no. 12, pp. 5283–5295, Dec. 2013.
[284] J. D. Ballester-Berman, J. M. López-Sánchez, and J. Fortuny-Guasch, "Retrieval of biophysical parameters of agricultural crops using polarimetric SAR interferometry," *IEEE Trans. Geosci. Remote Sens.*, vol. 43, no. 4, pp. 683–694, Apr. 2005.
[285] J. D. Ballester-Berman, J. M. Lopez-Sanchez, and M.-J. Sanjuan, "Determination of scattering mechanisms inside rice plants by means of PCT and high resolution radar imaging," in *Proc. 2009 IEEE Int. Geosci. Remote Sens. Symp.*, vol. 5, 2009, pp. V-138–V-141.
[286] M. Pichierri, I. Hajnsek, and K. P. Papathanassiou, "A multibaseline Pol-InSAR inversion scheme for crop parameter estimation at different frequencies," *IEEE Trans. Geosci. Remote Sens.*, vol. 54, no. 8, pp. 4952–4970, Aug. 2016.
[287] M. Pichierri and I. Hajnsek, "On the estimation of agricultural crop height from Pol-InSAR data," *2015 IEEE Int. Geosci. Remote Sens. Sympo (IGARSS)*, Milan, pp. 3207–3210, 2015.
[288] C. C. Chew, E. E. Small, K. M. Larson, and V. U. Zavorotny, "Vegetation sensing using GPS-interferometric reflectometry: Theoretical effects of canopy parameters on signal-to-noise ratio data," *IEEE Trans. Geosci. Remote Sens.*, vol. 53, no. 5, pp. 2755–2764, May 2015.
[289] Q. Chen, D. Won, D. M. Akos, and E. E. Small, "Vegetation sensing using GPS Interferometric Reflectometry: Experimental results with a horizontally polarized antenna," *IEEE J. Sel. Topics Appl. Earth Observ. Remote Sens.*, vol. 9, no. 10, pp. 4771–4780, Oct. 2016.
[290] W. Wan, K. M. Larson, E. E. Small, C. C. Chew, and J. J. Braun, "Using geodetic GPS receivers to measure vegetation water content," *GPS Solutions*, vol. 19, no. 2, pp. 237–248, 2015.
[291] K. P. Hunt, J. J. Niemeier, L. K. da Cunha, and A. Kruger, "Using cellular network signal strength to monitor vegetation characteristics," *IEEE Geosci. Remote Sens. Lett.*, vol. 8, no. 2, pp. 346–349, Mar. 2011.
[292] G. Baroni and S. Oswald, "A scaling approach for the assessment of biomass changes and rainfall interception using cosmic-ray neutron sensing," *J. Hydrol.*, vol. 525, pp. 264–276, 2015.
[293] T. E. Franz *et al.*, "Ecosystem-scale measurements of biomass water using cosmic ray neutrons," *Geophys. Res. Lett.*, vol. 40, no. 15, pp. 3929–3933, 2013.

Susan Catherine Steele-Dunne received the S.M. and Ph.D. degrees in hydrology from the Massachusetts Institute of Technology, Cambridge, MA, USA, in 2002 and 2006, respectively.

Since 2008, she has been with the Water Resources Section, Faculty of Civil Engineering and Geosciences, Delft University of Technology, Delft, The Netherlands. Her research interests include remote sensing, data assimilation, land atmosphere interactions, and land surface modeling.

Dr. Steele-Dunne is a member of the American Meteorological Society and the American Geophysical Union. She has also served the American Geophysical Union Hydrology Section as a member of the Remote Sensing Technical Committee and the Hydrological Sciences Award Committee, and the American Meteorological Society as a member of the Hydrology Committee.

Heather McNairn received the Bachelor of Environmental Studies degree from the University of Waterloo, Waterloo, Canada, in 1987, the Masters degree in soil science from the University of Guelph, Guelph, Canada, in 1991, and the Ph.D. degree in geography from Universit Laval, Quebec City, Canada, in 1999.

She is a Senior Scientist with Agriculture and Agri-food, Ottawa, Canada. She has 25 years of experience researching methods to monitor crops and soil using multispectral, hyperspectral, and synthetic aperture radar sensors. She is also an Adjunct Professor with the University of Manitoba, Winnipeg, Canada and Carleton University, Ottawa.

Alejandro Monsivais-Huertero (S'06–M'07–SM'13) received the B.S. degree in telecommunications engineering from the National Autonomous University of Mexico, Mexico City, Mexico, in 2002 and the M.S. degree in microwaves and optical telecommunications and the Ph.D. degree in microwaves, electromagnetism, and optoelectronics from the University of Toulouse, Toulouse, France, in 2004 and 2007, respectively.

From 2004 to 2006, he was with the Antennes, Dispositifs et Matriaux Microondes Laboratory, and from 2006 to 2007, with the Laboratoire d'Etudes et de Recherche en Imagerie Spatiale et Mdicale, both at the University of Toulouse. From 2008 to 2009, he was as a Postdoctorate Research Associate with the Center for Remote Sensing, Department of Agricultural and Biological Engineering, University of Florida, Gainesville, FL, USA. Since 2010, he has been working as a Researcher with the Superior School of Mechanical and Electrical Engineering campus Ticoman of the National Polytechnic Institute of Mexico, Mexico City. His research interests include microwave and millimeter-wave radar remote sensing, electromagnetic wave propagation, and retrieval algorithms.

Jasmeet Judge (S'94–M'00–SM'05) received the Ph.D. degree in electrical engineering and atmospheric, oceanic, and space sciences from the University of Michigan, Ann Arbor, MI, USA, in 1999.

She is currently the Director of the Center for Remote Sensing and an Associate Professor in the Agricultural and Biological Engineering Department, Institute of Food and Agricultural Sciences, University of Florida, Gainesville, FL, USA. Her research interests include microwave remote sensing applications to terrestrial hydrology for dynamic vegetation, data assimilation, modeling of energy and moisture interactions at the land surface and in the vadose zone, and spatiotemporal scaling of remotely sensed observations in heterogenous landscapes.

Dr. Judge is the Chair of the National Academies Committee on Radio Frequencies and a member of the Frequency Allocations in Remote Sensing Technical Committee in the the IEEE Geoscience and Remote Sensing Society.

Pang-Wei Liu (S'09–M'13) received the Ph.D. degree in agricultural engineering with a minor in electrical engineering from the University of Florida, Gainesville, FL, USA, in 2013.

He is currently a Postdoctoral Research Associate with the Center for Remote Sensing, Institute of Food and Agricultural Sciences, University of Florida. His research interests include modeling of active and passive microwave remote sensing for soil moisture and agricultural crops under dynamic hydrologic and vegetation conditions, data assimilation with crop growth models, application of LiDAR for forest biomass, and GNSS-R remote sensing for terrestrial applications. Dr. Liu is a member of the IEEE Geoscience and Remote Sensing Society and American Geophysical Union.

Kostas Papathanassiou (A'01–M'06–SM'09–F'13) received the Dipl.Ing. (Hons.) and Dr. (Hons.), both in Physics from the Graz University of Technology, Graz, Austria, in 1994 and 1999, respectively.

From 1992 to 1994, he was with the Institute for Digital Image Processing, Joanneum Research, Graz. Between 1995 and 1999, he was with the Microwaves and Radar Institute, German Aerospace Center (DLR-HR), Wessling, Germany. From 1999 to 2000, he was a European Union Postdoctoral Fellow with Applied Electromagnetics, St. Andrews, U.K. Since October 2000, he has been a Senior Scientist with DLR-HR, leading the Information Retrieval Research Group. His main research interests include polarimetric and interferometric processing and calibration techniques, polarimetric SAR interferometry, and the quantitative parameter estimation from SAR data, as well as in SAR mission design and SAR mission performance analysis.

Dr. Papathanassiou received the IEEE Geoscience and Remote Sensing Society International Geosicence and Remote Sensing Symposium Prize Award in 1998, the Best Paper Award of the European Synthetic Aperture Radar Conference in 2002, the German Aerospace Center (DLR) Science Award in 2002, and the DLR Senior Scientist Award in 2011. He is a member of DLR's TanDEM-X and Tandem-L Science Teams, Japan Aerospace Exploration Agency (JAXA)'s Advanced-Land-Observing-Satellite-2 Cal-Val teams, European Space agency's BIOMASS mission Advisory Group, SAOCOM-CS Expert Team, JAXA's Carbon and Kyoto Initiative, and NASA's Global Ecosystem Dynamics Investigation Lidar Mission Science Team.